Coordination Chemistry Reviews, 109 (1991) 125–180
Elsevier Science Publishers B.V., Amsterdam

STEREOSELECTIVITY IN ELECTRON TRANSFER REACTIONS INVOLVING METAL ION COMPLEXES

A. GRAHAM LAPPIN and ROSEMARY A. MARUSAK

Department of Chemistry and Biochemistry, University of Notre Dame, Notre Dame, IN 46556 (U.S.A.)

(Received 16 July 1990)

CONTENTS

A. INTRODUCTION

The intimate mechanisms of electron transfer between metal-ion complexes in solution have been a source of intense study for the past four decades. Two fundamental mechanistic types, inner-sphere and outer-sphere, have been identified [1]. In inner-sphere reactions, the primary coordination-spheres of the electron acceptor, A^{ox}, and donor, B^{red}, are linked by a bridging chromophore in an intermediate complex which is a precursor to electron transfer (eqn. (1)). This bridge may be a single atom or group of atoms and

0010–8545/91/$19.60

electron transfer takes place through the bridge (eqn. (2)) to give a successor complex as a second intermediate. The bridge itself may or may not be transferred in the overall reaction, depending on the relative labilities of the two reaction products (eqn. (3)).

$$[\mathrm{A}^{\mathrm{ox}}] + [\mathrm{B}^{\mathrm{red}}] \rightleftharpoons [\mathrm{A}^{\mathrm{ox}}\text{–}\mathrm{B}^{\mathrm{red}}] \tag{1}$$

$$[\mathrm{A}^{\mathrm{ox}}\text{–}\mathrm{B}^{\mathrm{red}}] \rightarrow [\mathrm{A}^{\mathrm{red}}\text{–}\mathrm{B}^{\mathrm{ox}}] \tag{2}$$

$$[\mathrm{A}^{\mathrm{red}}\text{–}\mathrm{B}^{\mathrm{ox}}] \rightleftharpoons [\mathrm{A}^{\mathrm{red}}] + [\mathrm{B}^{\mathrm{ox}}] \tag{3}$$

In outer-sphere reactions, the primary coordination spheres remain intact during the electron transfer process. Outer-sphere precursor complex assembly takes place (eqn. (4)) prior to electron transfer which, in most instances, is presumed to involve weak overlap between donor and acceptor orbitals (eqn. (5)). Dissociation of the successor complex is generally rapid (eqn. (6)) and does not participate in the rate-limiting step.

$$[\mathrm{A}^{\mathrm{ox}}] + [\mathrm{B}^{\mathrm{red}}] \rightleftharpoons [\mathrm{A}^{\mathrm{ox}},\mathrm{B}^{\mathrm{red}}] \tag{4}$$

$$[\mathrm{A}^{\mathrm{ox}},\mathrm{B}^{\mathrm{red}}] \rightarrow [\mathrm{A}^{\mathrm{red}},\mathrm{B}^{\mathrm{ox}}] \tag{5}$$

$$[\mathrm{A}^{\mathrm{red}},\mathrm{B}^{\mathrm{ox}}] \rightleftharpoons [\mathrm{A}^{\mathrm{red}}] + [\mathrm{B}^{\mathrm{ox}}] \tag{6}$$

Both inner-sphere and outer-sphere reactions are generally characterized as very simple kinetic processes and so detailed mechanistic information is rather difficult to obtain. Mechanistic information can be supplemented by product analysis where kinetic rather than thermodynamic control governs, and this has proven to be immensely important in understanding inner-sphere processes [1–3], but much less so in the case of outer-sphere reactions where the reactions themselves involve no bond breaking.

The fact that no bonds are made or broken during outer-sphere electron transfer processes has made them amenable to theoretical treatment [1,4–6]. Although sophisticated quantum mechanical calculations have met with some success [7–9], the most widely used approach involves the use of the Marcus linear free energy correlation [4,5] expressed in eqns. (7) and (8) where $\Delta G^{**}_{\mathrm{AB}}$ is the electrostatically corrected free energy of activation and ΔG° is the electrostatically corrected free energy change for the reaction between A^{ox} and $\mathrm{B}^{\mathrm{red}}$. The quantity $\Delta G^{**}_{\mathrm{AA}}$ refers to the free energy of activation for the self-exchange reaction between A^{ox} and $\mathrm{A}^{\mathrm{red}}$, $\Delta G^{**}_{\mathrm{BB}}$ is the corresponding value for reagent B.

$$\Delta G^{**}_{\mathrm{AB}} = \tfrac{1}{2}[\Delta G^{**}_{\mathrm{AA}} + \Delta G^{**}_{\mathrm{BB}} + \Delta G^{\circ}\ (1 + \alpha^{**})] \tag{7}$$

$$\alpha^{**} = \frac{\Delta G^{\circ}}{4\ (\Delta G_{\mathrm{AA}} + \Delta G^{**}_{\mathrm{BB}})} \tag{8}$$

The electrostatic correction [10] involves the calculation of work terms, $\omega(r)$, for the approach of charged reactants in the reaction medium and is generally represented by

$$\omega_{AB}(r)=\frac{z_A z_B e^2}{D_s r(1+\beta r)} \tag{9}$$

where D_s is the static dielectric constant for the medium, $\beta=(8\pi Ne^2/1000D_s kT)^{1/2}$, z_A and z_B are the charges on the reactants, and r is the distance of approach between the reactants, generally assumed to be the sum of the radii, a_A+a_B. Where the reactants are not spherically symmetric, some idea of shape can be introduced by approximating the species as a spheroid with axes of length d_x, d_y, and d_z, such that the radius is given by

$$a=\tfrac{1}{2}(d_x d_y d_z)^{1/3} \tag{10}$$

This treatment involves some tacit assumptions about the distance and orientation of approach of the reagents, namely that electron transfer takes place on contact between the reactants and that there are no orientation effects. This is not necessarily the case, and a number of workers have modified this framework in attempts to deduce information about both orientation and distance. For example, a steric factor can be included [11].

The very features which are attractive from the point of view of theory present the greatest difficulties with the detailed determination of mechanism. It has been pointed out [1] that information on the proximity of the reactants and on the reactant orientation required for efficient electron transfer is difficult to obtain in outer-sphere reactions. Such information is more generally available for inner-sphere reactions because of the special nature of the bridging chromophore.

There are a number of experimental [12–16] and theoretical [17,18] approaches which have been used in an attempt to answer questions about electron transfer distance and orientation in outer-sphere reactions. One experimental approach, stereoselectivity, forms the subject of this review. It is only within the last decade that experiments in electron transfer stereoselectivity have been carried out with some success, due principally to a more complete understanding of the substitution and electron transfer behavior of the reagents. Results to date have been intriguing, however detailed interpretation remains difficult. This review will highlight these difficulties and suggest new approaches.

B. CHIRALITY IN METAL-ION COMPLEXES

Chiral molecules are most readily defined as those which have no mirror plane and no inversion center. The simplest example is the tetrahedral center with four dissimilar binding groups (Fig. 1) found most frequently at saturated carbon and coordinated nitrogen but also a possible geometry for metal-ion complexes. The bulk of examples in this review are metal-ion complexes with geometry based on an octahedron where chirality arises from the placement of chelate rings.

Tris-bidentate chelate complexes (Fig. 2) have differing helicities along their C_3 and C_2 axes. The configuration is designated in terms of the C_3 axis as Δ if there is a clockwise or plus, $P(C_3)$, rotation and Λ if there is a counter-clockwise or minus, $M(C_3)$, rotation. More formally [19], the configuration of the chelate rings is defined in terms of the helicity exhibited by the pairs of edges of the octahedron which contain chelate rings (Fig. 3). Each pairwise

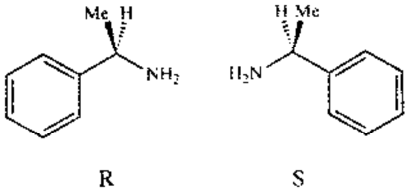

Fig. 1. (*S*) and (*R*) configurations of 1,1-amino-phenylethane.

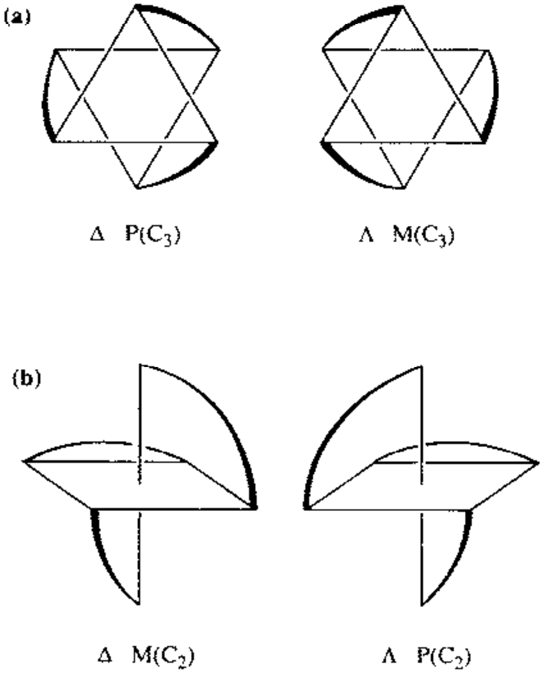

Fig. 2. Representations of the Δ and Λ configurations for a tris-bidentate chelate complex viewed along (a) the C_3 axis and (b) the C_2 axis.

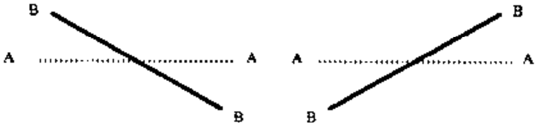

(a) Δ or δ (b) Λ or λ

Fig. 3. The skew arrangement of bonds which define (a) Δ and (b) Λ helical arrangements. The dotted line AA is in the plane of the paper while the full line BB is above the plane.

interaction is noted, and thus a Δ-tris chelate is described as ΔΔΔ, abbreviated to Δ [20], and other chelate arrangements can be described in a consistent fashion.

Chelate ring conformation also provides a source of optical activity. For a five-membered, saturated chelate ring there are two favorable conformations, one where the C–C bond lies parallel to the C_3 axis, the *lel* conformation, the other where the C–C bond lies oblique to this axis, the *ob* conformation. In Fig. 4, these two conformations are illustrated for the 1,2-diaminoethane ring of a Λ tris-chelate. The helicity of the *lel* is clockwise or *δ*, while that of the *ob* is counter-clockwise or *λ*. Full designation of the chirality of the tris-chelate requires that the helicity of all three rings be specified and thus an isomer with one parallel and two oblique rings, *lelob*$_2$, is Δ(*δλλ*) and its enantiomer is Δ(λδδ). In this review the *lel*/*ob* designation is preferred and there are four possible diastereomeric pairs; *lel*$_3$, *lel*$_2$*ob*, *lelob*$_2$, and *ob*$_3$.

The diastereoselectivity involved when chiral chelate ligands bind to an octahedral metal center also figures prominently in the work discussed in this review. Such diastereomers frequently differ significantly in energy, producing stereoselective or even stereospecific ligand binding processes. Perhaps

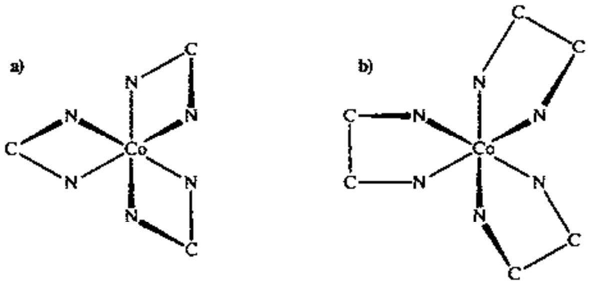

Λ (δδδ) ***lel*$_3$** Λ (λλλ) ***ob*$_3$**

Fig. 4. Chelate ring conformations shown for the (a) (*lel*$_3$)-Λ(*δδδ*) and (b) (*ob*$_3$)-Λ(*λλλ*) isomers of $[Co(en)_3]^{2+}$.

the best known example [21] of this is the binding of R-pdta^{4-} which leads exclusively to the Δ configuration at the metal center.

Some comment is required about the availability of absolute configuration data for metal-ion complexes. This information is crucial to the interpretation and understanding of stereoselectivity experiments. While there is now a large body of unambiguous assignments of absolute configurations [22], this is not universally true for all the complexes discussed in this review. Where ambiguities exist, the most widely accepted configurations are quoted.

C. CHIRAL INDUCTION IN OUTER-SPHERE REACTIONS BETWEEN METAL-ION COMPLEXES

Stereoselectivity in outer-sphere electron transfer reactions is a direct measure of the relative reactivities of an optically active reagent, $\Delta\text{–A}^{\text{ox}}$, with the enantiomeric forms of the electron transfer reaction partners $\Delta\text{–B}^{\text{red}}$ and $\Lambda\text{–B}^{\text{red}}$, and is generally expressed as enantiomeric excess.

$$\Delta\text{–A}^{\text{ox}} + \Delta\text{–B}^{\text{red}} \rightarrow \Delta\text{–A}^{\text{red}} + \Delta\text{–B}^{\text{ox}} \quad k_{\Delta\Delta} \tag{11}$$

$$\Delta\text{–A}^{\text{ox}} + \Lambda\text{–B}^{\text{red}} \rightarrow \Delta\text{–A}^{\text{red}} + \Lambda\text{–B}^{\text{ox}} \quad k_{\Delta\Lambda} \tag{12}$$

The information obtained serves as a sensitive probe of the geometry of intermediates or transition states along the reaction coordinate.

Two techniques are usually employed for detecting chiral induction in electron transfer reactions. The first is the observation of rate differences in reactions of enantiomeric reaction partners with an optically active complex. In general, this is indicated by differences in the rate constants $k_{\Delta\Delta}$ and $k_{\Delta\Lambda}$, and requires that both oxidant and reductant can be isolated in enantiomeric forms. Alternatively, if one reagent cannot be prepared in enantiomeric forms, stereoselectivity can be measured kinetically by the detection of rate differences in the parallel reactions with the racemic mixture, provided the rate of interconversion of the enantiomers is slow relative to the electron transfer process. The second technique is the detection of chiral induction in the kinetic products of the reaction between an optically active complex and a racemic mixture. This method has its own set of constraints and generally requires that the rate of interconversion of isomers in the racemate is fast relative to electron transfer. For outer-sphere reactions, this method is generally a more sensitive means for obtaining results.

(i) Historical aspects

Early work on electron-transfer stereoselectivity was fraught with difficulties, principally the result of a lack of information about the self-exchange rates of the reagents and their substitution behavior. Adamson and Spees [23] failed to detect chiral induction in $[Cr(bpy)_3]^{3+}$ formed in the oxidation of $[Cr(bpy)_3]^{2+}$ by optically active $[Co(en)_3]^{3+}$ (eqn. (13)), and correctly realized that this result could be explained either by the absence of stereoselectivity in the reaction or by rapid racemization of the $[Cr(bpy)_3]^{3+}$. Grossman and Wilkins [24] outlined a mechanism for this rapid racemization, citing the combination of the lability in $[Cr(bpy)_3]^{2+}$ and the high self-exchange rate for the $[Cr(bpy)_3]^{3+/2+}$ system [25]. These workers attempted to measure rate differences in reactions of enantiomeric cobalt(III) complexes with a single diastereomer of $[Fe(pdta)]^{2-}$ where chirality around the labile iron(II) center is dictated by the chiral center on the ligand backbone. Rate differences for the enantiomers were within the limits of experimental error, (Table 1), a disappointing observation since this kinetic method had been used in the detection of electron transfer stereoselectivity in two organic reactions [26,27].

$$[Co(en)_3]^{3+} + [Cr(bpy)_3]^{2+} \rightarrow [Cr(bpy)_3]^{3+} + [Co(en)_3]^{2+} \tag{13}$$

Considerable interest was generated when Sutter and Hunt reported [28] that $[Cr(phen)_3]^{3+}$, formed in the oxidation of $[Cr(phen)_3]^{2+}$ by a stoichiometric amount of $[\Delta\text{-}Co(phen)_3]^{3+}$, showed an enantiomeric excess of 84% of the Λ-isomer

$$[\Delta\text{-}Co(phen)_3]^{3+} + [Cr(phen)_3]^{2+} \rightarrow [\Lambda\text{-}Cr(phen)_3]^{3+} + [Co(phen)_3]^{2+} \tag{14}$$

The result supported the concept that electron transfer is accompanied by an intimate interaction between the complexes and was the subject of studies to provide a detailed explanation of the mechanism of chiral induction. Hückel calculations reveal [29] that the electron spin density is greatest at the 4 and 7 positions of the phenanthroline ring, making them 'active sites' for electron transfer. Overlap of the orbitals at the 4 and 7 positions is optimized by interactions along the C_3 axes of the complexes, resulting in the observed stereoselectivity.

Unfortunately, attempts to reproduce the experimental observations encountered difficulties. Kane-Maguire et al. recognized [30] that, under conditions of excess $[Co(phen)_3]^{3+}$ oxidant, a rapid rate of racemization of the reductant is a prerequisite to the detection of stereoselectivity and adjusted conditions to favor this but with no success. In fact [31], the rate of racemization of $[Cr(phen)_3]^{2+}$ is comparatively slow, $0.123\ s^{-1}$, while the electron transfer is fast [32], and so both enantiomers will be oxidized under the conditions of excess oxidant, preventing the detection of any chiral induction. Kane-Maguire et al. also examined a variety of other reactions, mostly with chromium(II) reductants (Table 2) but could detect no stereoselectivity and

TABLE 1

Rate data from ref.24 indicating the absence of chiral induction in electron transfer reactions at 25°C and 0.5 M ionic strength, pH ~4.5

Reductant	Oxidant	k (M^{-1} s^{-1})	ΔH^* (kcal mol^{-1})	ΔS^* (cal K^{-1} mol^{-1})
$[\Lambda\text{-Fe}(S\text{-pdta})]^{2-}$	$[\Delta\text{-Co(edta)}]^{-}$	12.5	6.7	−32
$[\Lambda\text{-Fe}(S\text{-pdta})]^{2-}$	$[\Lambda\text{-Co(edta)}]^{-}$	13.0	7.5	−29
$[\Lambda\text{-Fe}(S\text{-pdta})]^{2-}$	$[\Delta\text{-Co(edta)Cl}]^{2-}$	3.9×10^2	6.3	−26
$[\Lambda\text{-Fe}(S\text{-pdta})]^{2-}$	$[\Lambda\text{-Co(edta)Cl}]^{2-}$	3.9×10^2	6.5	−25
$[\Lambda\text{-Fe}(S\text{-pdta})]^{2-}$	$[rac\text{-Co(ox)}_3]^{3-}$	2.2×10^2	3.0	−37
$[\Lambda\text{-Co}(S\text{-pdta})]^{2-}$	$[rac\text{-Fe(bpy)}_3]^{3+}$	8.1×10^4	5.7	−17
$[\Lambda\text{-Fe}(S\text{-pdta})]^{2-}$	$[rac\text{-}cis\text{-Co(en)}_2(NH_3)Cl]^{2+}$	2.0×10^2	10.9	−12
$[rac\text{-Fe(pdta)}]^{2-}$	$[Co(NH_3)_5Cl]^{2+}$	2.2×10^3	9.2	−13
$[rac\text{-Fe(pdta)}]^{2-}$	$[Co(NH_3)_5Br]^{2+}$	1.8×10^3	10.9	−7
$[rac\text{-Fe(pdta)}]^{2-}$	$[Co(NH_3)_5N_3]^{2+}$	7.0×10^3	8.6	−12
$[rac\text{-Fe(pdta)}]^{2-}$	$[Co(NH_3)_5NCS]^{2+}$	2.7×10^{-1}		

±15% deviation would be detected in reactions with racemic complexes.

TABLE 2

Electron transfer reactions reported in ref.30 to show no chiral induction

Oxidant	Reductant
$[\Lambda\text{-}(+)\text{-Co(phen)}_3]^{3+}$	$[\text{Cr(phen)}_3]^{2+}$
$[\Lambda\text{-}(+)\text{-Co(phen)}_3]^{3+}$	$[\text{Cr(bpy)}_3]^{2+}$
$[\Delta\text{-}(-)\text{-Co(bpy)}_3]^{3+}$	$[\text{Cr(phen)}_3]^{2+}$
$[\Delta\text{-}(-)\text{-Co(bpy)}_3]^{3+}$	$[\text{Cr(bpy)}_3]^{2+}$
$[\Lambda\text{-}(+)\text{-Co(phen)}_2\text{(en)}]^{3+}$	$[\text{Cr(phen)}_3]^{2+}$
$[\Lambda\text{-}(+)\text{-Co(phen)(en)}_2]^{3+}$	$[\text{Cr(phen)}_3]^{2+}$
$[\Lambda\text{-}(+)\text{-Co(en)}_3]^{3+}$	$[\text{Cr(phen)}_3]^{2+}$
$[\Lambda\text{-}(+)\text{-Co(phen)}_3]^{3+}$	$[\text{Cr(en)}_3]^{2+}$
$[\Lambda\text{-}(+)\text{-Co(phen)}_3]^{3+}$	$[\text{Cr(edta)}]^{2-}$
$[\Delta\text{-}(+)\text{-Co(edta)}]^{-}$	$[\text{Cr(phen)}_3]^{2+}$
$[\Delta\text{-}(+)\text{-Co(edta)}]^{-}$	$[\text{Cr(bpy)}_3]^{2+}$
$[\Delta\text{-}(+)\text{-Co(}R(+)\text{-cysu)}_3]^{3-}$	$[\text{Cr(bpy)}_3]^{2+}$
$[\Delta\text{-}(+)\text{-Co(edta)}]^{-}$	$[\text{Cr(edta)}]^{2-}$

pointed to this as 'strong evidence for the general absence of stereospecific effects in outer-sphere redox processes'.

This generalized conclusion had the effect of discouraging further work on electron-transfer stereoselectivity. Indeed, in the next year, Yoneda and co-workers reported [33] that $[\text{Co(acac)}_3]$ formed in the oxidation of $[\text{Co(acac)}_3]^-$ by $[\Lambda\text{-Co(bpy)}_3]^{3+}$ has an enantiomeric excess of 4.84% of the Δ isomer, but declined to interpret their observations in terms of a stereoselective electron transfer, preferring instead an explanation involving the Pfeiffer effect. It was proposed that a stereochemical preference, or Pfeiffer effect, is induced in the labile $[\text{Co(acac)}_3]^-$ by association with $[\Lambda\text{-Co(bpy)}_3]^{3+}$, and so the chiral induction does not require stereoselectivity in the electron transfer step. Reduction of $[\text{Co(acac)}_3]$ by $[{}^*\text{Ru(bpy)}_3]^{2+}$ was, however, reported [34] to be a stereoselective process.

The prevalence of stereoselectivity was pinpointed succinctly by Geselowitz and Taube [35] who recognized the technical difficulties of measuring small rate differences in rates of reactions of diastereomeric pairs, and that the detection of chiral induction in a kinetic product is a much more sensitive method. In the reactions examined by Kane-Maguire et al., detection of chiral induction was attempted by measuring optical activity in 'inert' oxidized products. However, if for example, optically active $[\text{Cr(phen)}_3]^{3+}$ is formed when $[\Lambda\text{-Co(phen)}_3]^{3+}$ is reduced by an excess of labile $[\text{Cr(phen)}_3]^{2+}$, a complication arises. Racemization of the $[\text{Cr(phen)}_3]^{3+}$ can occur, not only by ligand exchange processes, but also by rapid electronic self-exchange with the more labile $[\text{Cr(phen)}_3]^{2+}$. Thus, the choice of suitable reagents as probes for stereoselective electron transfer is critical. Clearly reagents which are substitution inert and have low self-exchange rates with the labile form are good choices, and a number of suitable candidates are presented in Table 3. Geselowitz and Taube exploited this behavior in reactions with a variety of reagents.

A contributing factor to the development and understanding of stereoselective electron transfer reactions has been the concomitant increase in interest in chiral recognition between substitution inert metal-ion complexes in solutions. These studies are complementary and provide model information on stereochemical preferences of likely intermediates in the electron transfer reaction.

(ii) Ideal outer-sphere reagents: $[Co(edta)]^{-/2-}$ and $[Co(acac)_3]^{0/-}$

The preceding requirements for outer-sphere chiral induction make it possible to formulate a judicious choice of reaction partners and conditions to avoid problems such as rapid self-exchange racemization. Hence, a fairly large number of stereoselective reactions have been reported. Tris(1,10-phenanthroline) and tris(2,2′-bipyridyl) complexes have been used extensively in stereoselectivity studies with the two probe systems $[Co(edta)]^{-/2-}$ [35,44,45] and $[Co(acac)_3]^{0/-}$ [33,34]. These systems are ideal probes for stereoselectivity because the inert cobalt(III) forms are not subject to rapid self-exchange racemization. Both systems have provided some interesting and, at the same time, puzzling results. Work with reagents where there is no possibility for the formation of strong hydrogen bonds in electron transfer precursor complexes is emphasized in this section. Although precursor formation is expected to be weak in these systems, it can make a contribution to the overall chiral induction, and the interplay between effects due to the precursor and electron transfer steps is an important consideration. Other studies, where precursor formation is much better defined, are discussed in Sects. D and E.

Studies of the reactions of $[Co(acac)_3]^{0/-}$ are facilitated by the ease of

TABLE 3

Properties of reagents suitable as electron transfer stereoselectivity probes, 25.0°C

Reagent	k_{AA} (M^{-1} s^{-1})	E° (V)	k_{rac}[a] (s^{-1})	Ref.
$[Co(edta)]^{-/2-}$	1×10^{-7}	0.42	$\sim 10^6$	36–39
$[Co(acac)_3]^{0/-}$	--	--	--	Not available
$[Co(en)_3]^{3+/2+}$	3.2×10^{-5}	-0.18	3×10^3	40–42
$[Co(phen)_3]^{3+/2+}$	12	0.37	0.123	31, 43
$[Co(bpy)_3]^{3+/2+}$	20	0.32	~ 10	11, 31

[a] Rate of racemization of labile cobalt(II) form.

isolation of the neutral $[\mathrm{Co(acac)_3}]$ in dichloroethane or carbon tetrachloride. Yoneda and coworkers [33] examined the oxidation of $[\mathrm{Co(acac)_3}]^-$ by $[\Lambda\text{-}\mathrm{Co(phen)_3}]^{3+}$ and found a 4.8% enantiomeric excess of $[\Delta\text{-}\mathrm{Co(acac)_3}]$. Porter and Sparks [34,46] found that the photoinduced reduction of an excess of racemic $[\mathrm{Co(acac)_3}]$ by $[\Delta\text{-}{}^*\mathrm{Ru(bpy)_3}]^{2+}$ resulted in the formation of an excess of $[\Delta\text{-}\mathrm{Co(acac)_3}]$, indicating preferential reduction of the Λ isomer with a rate constant a factor of 1.03 greater than that of the Δ isomer. Although both these reactions show the same ΔΛ preference, interpretation of the results is not simple, and need not reflect a common explanation.

Reaction between $[\Lambda\text{-}\mathrm{Co(phen)_3}]^{3+}$ and the oppositely charged $[\mathrm{Co(acac)_3}]^-$ involves the formation of a moderately strong precursor complex which can be of importance in determining the stereoselectivity [33]. Also, the lability of the reductant allows for an induced stereochemical preference or Pfeiffer effect such that the equilibrium between Δ and Λ forms of $[\mathrm{Co(acac)_3}]^-$ is displaced in favor of the former isomer. An explanation involving the Pfeiffer effect is preferred by the authors of the work since oxidation of $[\mathrm{Co(acac)_3}]^-$ by $\mathrm{H_2O_2}$ in the presence of $[\Lambda\text{-}\mathrm{Ni(phen)_3}]^{2+}$ leads to the same stereochemical result [33]. However, it is worth noting that preferential ion-pair formation between the Λ-form of the metal phenanthroline complexes and $[\Delta\text{-}\mathrm{Co(acac)_3}]^-$ as an electron transfer precursor provides an explanation which is equally satisfactory.

A Pfeiffer effect is not possible in the reaction between $[\Delta\text{-}{}^*\mathrm{Ru(bpy)_3}]^{2+}$ and $[\mathrm{Co(acac)_3}]$ since both complexes are inert to substitution. Association with the neutral $[\mathrm{Co(acac)_3}]$ is expected to be weak. However, stereoselectivity in models for the electron transfer precursor has been examined for $[\mathrm{Ni(phen)_3}]^{2+}$ [47,48] and $[\mathrm{Ru(phen)_3}]^{2+}$ [49] by both solvent extraction and ion exchange chromatography. With both complex ions, the stereoselectivity in the association shows a preference for the ΔΔ interaction over that for ΔΛ, in contrast to the results of the electron transfer experiment. Quantitative comparisons can be made for the ruthenium case [49] where the association constant for the ΔΔ interaction is 3.86 and for the ΔΛ interaction it is 3.80 at 25°C. This result is contrary to simple dipolar calculations which predict a preferred ΔΛ interaction [50] and prompted a theoretical investigation by Mason and coworkers [51,52] in which an extended transition monopole model is used to calculate the average dispersion energies and chiral discrimination of the ΔΔ and ΔΛ interactions for two D_3 tris-(butadienyl) complexes which have similar extended π-systems and where computation is simplified. Although large discriminations are not obtained, the results suggest that differences in dispersion energies for the two interactions become greater as the separation distance is decreased and a slight preference for the ΔΔ interaction occurs at contact distances.

One interesting aspect of the stereoselective photoreduction of $[\mathrm{Co(acac)_3}]$

by [*Ru(bpy)$_3$]$^{2+}$ has been the appearance of reports [53,54] of reactions of derivatives of [*Ru(bpy)$_3$]$^{2+}$ in which chiral groups are attached to the periphery of the 2,2′-bipyridyl ligand (Fig. 5). Circular dichroism studies with [Ru(*S*(−)-PhEt-bpy)$_3$]$^{2+}$ indicate that the ligand binds stereospecifically to the metal center, inducing the Λ-configuration and that the enantiomeric ligand forms the Δ-configuration. Stereoselectivity increases with increasing proportion of ethanol in an aqueous/ethanol mixture and the ratio of rate constants reaches a maximum of 1.54 with the Λ photoreductant reacting more rapidly with the [Λ-Co(acac)$_3$] [53]. The selectivity is the opposite of that detected with the parent [*Ru(bpy)$_3$]$^{2+}$, implying that it is the ligand chirality and not the configuration around the metal center which is the determining feature. In a related study [54], the complex with ((1*R*,2*S*,5*R*)-(−)-menthylcarboxy)-2,2′-bipyridine, ((−)-mncb), shows no induced chirality at the metal center so that discrimination is effected by the peripheral menthol groups. In this case, the stereoselectivity shows a preference for reaction with [Δ-Co(acac)$_3$] with a rate constant ratio of 1.33 in 70% aqueous ethanol. Both of these complexes have increased resistance to the photoracemization found with [*Ru(bpy)$_3$]$^{2+}$ and are useful as photocatalysts.

By far the most generally used stereoselectivity probe has been the [Co(edta)]$^{-/2-}$ couple. Geselowitz and Taube [35] studied oxidations of

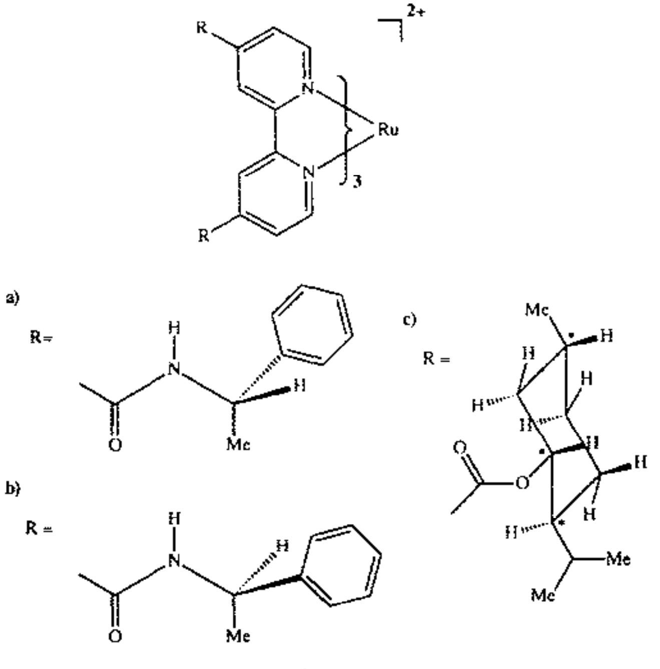

Fig. 5. Derivatives of [Ru(bpy)$_3$]$^{2+}$. (a) [Ru(*S*(−)-PhEt-bpy)$_3$]$^{2+}$; (b) [Ru(*R*(+)-PhEt-bpy)$_3$]$^{2+}$; (c) [Ru((−)-mncb)]$^{2+}$.

$[Co(edta)]^{2-}$ by $S_2O_8^{2-}$ catalyzed by a variety of optically active $[M(phen)_3]^{2+}$ and $[M(bpy)_3]^{2+}$ complexes. The rate-limiting step is outer-sphere electron transfer between the metal complexes and the method circumvents problems of racemization of the strongly oxidizing trivalent species. This work has been extended to include a number of other systems, including electron transfer quenching of the excited states of $[{}^*Ru(bpy)_3]^{2+}$ [44] and its chiral micellar derivative $[{}^*Ru((-)\text{-mncb})_2(bpy\text{-}C_{12})]^{2+}$ [55] where differences in reactivity are sufficiently large to allow kinetic detection, and the copper(I) derivative $[{}^*Cu(2,9\text{-}Me_2phen)(R,R\text{-diop})]^+$ (*R*,*R*-diop = (*R*,*R*)-2,3-O-isopropylidene-2,3-dihydroxy-1,4-bis(diphenylphosphino)butane) where both kinetic and product analysis studies provide complementary information [56]. An interesting feature of the reaction with $[{}^*Ru(bpy)_3]^{2+}$ is the presence of a marked solvent effect. In aqueous solution where the reactions are diffusion-controlled, there is no discrimination, suggesting that the chiral induction takes place in contact ion pairs which are more prevalent in ethanolic solutions where stereoselectivity is as large as 6%. Detailed studies with derivatives of $[Co(en)_3]^{2+}$ [57–60] and with bis(oxime-imine) complexes of nickel(IV) [61–63] have also been reported but these are thought to involve hydrogen bonding interactions and will be discussed in separate sections.

While results with $[Co(acac)_3]^{0/-}$ and $[Co(edta)]^{-/2-}$ are readily obtained, interpretation of the data presents quite a different problem. Stereoselectivity or chiral induction can arise from a shape selectivity in the formation of the precursor to electron transfer, chiral recognition, or from an electronic effect, the result of differences in orbital overlap or rearrangement energy in the electron transfer process itself. Reference to the collected data, Table 4, reveals that, with reagents of similar shape and configuration, the stereoselectivities appear random and show no apparent correlation with electronic structure. A number of authors have speculated on the source of the stereoselectivity and there would appear to be a preference for an explanation involving rearrangements within the diffusion-controlled precursors, but the evidence is not compelling.

(iii) Reactions between $[M(phen)_3]^{3+/2+}$ *and* $[M(bpy)_3]^{3+/2+}$

The electron self-exchange rate for $[Co(phen)_3]^{3+/2+}$ has been measured by the $[Co(phen)_3]^{2+}$ catalyzed racemization of optically active $[Co(phen)_3]^{3+}$ and compared with results of radiotracer studies [43]. It is concluded that any stereoselectivity in the reaction is small. Chiral induction has been observed in the cross-reaction between $[\Delta\text{-}Co(phen)_3]^{3+}$ and $[Co(4,7\text{-}Me_2phen)_3]^{2+}$ (Fig. 6) in nitrate media and is estimated to be ≈15% ΔΛ, not sufficiently large to have a dramatic effect on rate measurements. The reaction rates show a strong anion dependence and there is kinetic

TABLE 4

Stereoselective electron transfer and ion-pairing interactions involving $[Co(edta)]^{-/2-}$ and $[Co(acac)_3]^{0/-}$ in aqueous solution at 25°C

Oxidant	Reductant	Stereoselectivity				Ref.
		ET		IP		
		$k_{\Delta\Lambda}/k_{\Delta\Delta}$	Pref.	$K_{\Delta\Lambda}/K_{\Delta\Delta}$	Pref.	
$[Ni(phen)_3]^{2+}$	$[Co(acac)_3]^-$				$\Delta\Lambda$	33
$[Co(phen)_3]^{3+}$	$[Co(acac)_3]^-$	1.10	$\Delta\Lambda$			33
$[Co(acac)_3]$	$[{}^*Ru(bpy)_3]^{2+}$	1.08	$\Delta\Lambda$			34
$[Co(acac)_3]$	$[{}^*Ru(bpy)_3]^{2+}$	1.03	$\Delta\Lambda$			46
$[Co(acac)_3]$	$[{}^*Ru(S(-)\text{-PhEtbpy})_3]^{2+}$	0.65	$\Delta\Delta$[a]			53
$[Co(acac)_3]$	$[{}^*Ru((-)\text{-mncb})_3]^{2+}$	1.33	$\Delta\Lambda$[b]			54
$[Co(acac)_3]$	$[Ni(phen)_3]^{2+}$				$\Delta\Delta$	47, 48
$[Co(acac)_3]$	$[Ru(phen)_3]^{2+}$			0.98	$\Delta\Delta$	49
$[Fe(bpy)_3]^{3+}$	$[Co(edta)]^{2-}$		$\Delta\Lambda$			35
$[Fe(phen)_3]^{3+}$	$[Co(edta)]^{2-}$		$\Delta\Lambda$			35
$[Ru(bpy)_3]^{3+}$	$[Co(edta)]^{2-}$	1.01	$\Delta\Lambda$[c]			35
$[Os(bpy)_3]^{3+}$	$[Co(edta)]^{2-}$	0.90	$\Delta\Delta$[c]			35
$[Co(bpy)_3]^{3+}$	$[Co(edta)]^{2-}$		$\Delta\Delta$			35
$[Co(phen)_3]^{3+}$	$[Co(edta)]^{2-}$	0.87	$\Delta\Delta$			45
$[Co(edta)]^-$	$[{}^*Ru(bpy)_3]^{2+}$		$\Delta\Lambda$[d]			44
$[Co(edta)]^-$	$[{}^*Ru((-)\text{-mncb})_2(bpyC_{12})]^{2+}$		$\Delta\Lambda$[e]			55
$[Co(edta)]^-$	$[{}^*Cu(R,R\text{-diop})(dmp)]^+$		$\Delta\Lambda$[d]			56
$[Co(en)_2(gly)]^+$	$[{}^*Ru(bpy)_3]^{2+}$		[e]			64

[a] 90% ethanol.
[b] 70% EtOH.
[c] $S_2O_8^{2-}$, pH 2.1.
[d] 90% methanol, $\Delta = R,R$.
[e] No discrimination detected.

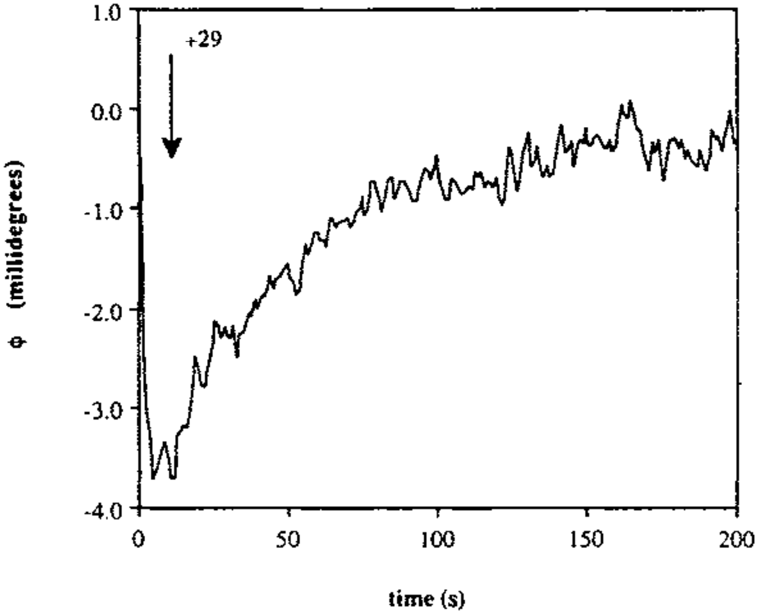

Fig. 6. Decay of the circular dichroism signal at 487 nm for $[Co(4,7\text{-}Me_2phen)_3]^{3+}$ formed in the oxidation of [*rac*-$Co(4,7\text{-}Me_2phen)_3]^{2+}$ by $[\Lambda\text{-}Co(phen)_3]^{3+}$ at 25.0°C and 0.10 M ionic strength (NO_3^-). (Reproduced with permission from ref. 43.)

evidence for the formation of ion-multiplets as intermediates in the electron transfer process. Association between $[Ru(phen)_3]^{2+}$ complexes in ion-multiplets has been noted in NMR studies [65,66] and the ΔΛ aggregate is found to be more compact than the ΔΔ aggregate (Fig. 7), consistent with an important role for discrimination within these structures. These solution structures bear some resemblance to the packing of the complexes in crystalline lattices [67,68]. Chiral discrimination has also been noted with racemic pairs which are preferentially absorbed on montmorillonite clays [69–71]. Attempts to produce chiral electrodes have also been reported. When an SnO_2 electrode is coated with montmorillonite clay in which $[\Delta\text{-}Ru(bpy)_3]^{2+}$ has been incorporated, $[\Lambda\text{-}Co(phen)_3]^{2+}$ is oxidized at a greater rate than $[\Delta\text{-}Co(phen)_3]^{2+}$ to produce a 7% enantiomeric excess [72,73].

D. REACTIONS INVOLVING METAL BIS(OXIME-IMINE) COMPLEXES

Complexes with derivatives of sexidentate bis(oxime-imine) ligands (Fig. 8) have yielded some intriguing kinetic and stereoselectivity studies. These ligands provide a stabilizing environment for low-spin d^6 ions and a number of redox couples have been investigated, including $[Ni^{IV/III}Me_2L(1)]^{2+/+}$

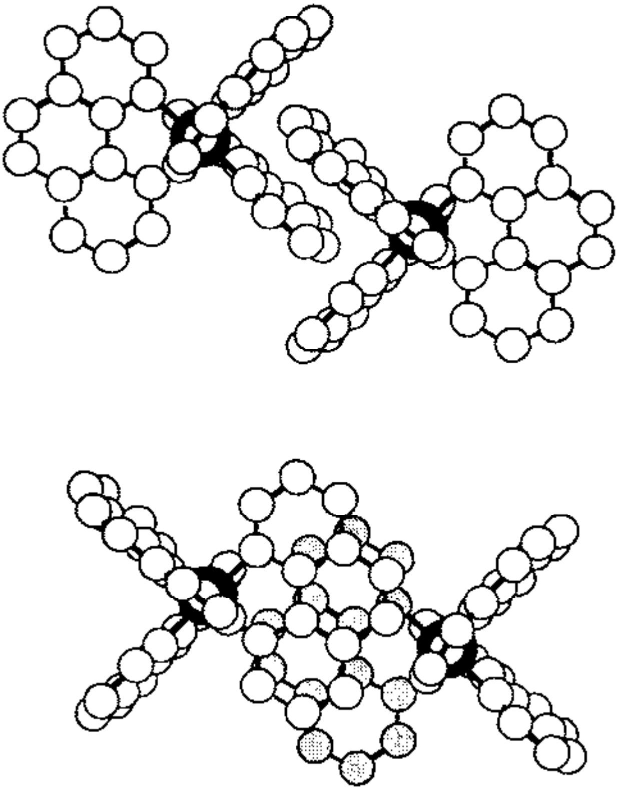

Fig. 7. Schematic representation of the ion pair complexes formed between Δ- and Λ-$[Ru(phen)_3]^{2+}$ ions as determined by NMR studies. (Modified from refs. 65 and 66.)

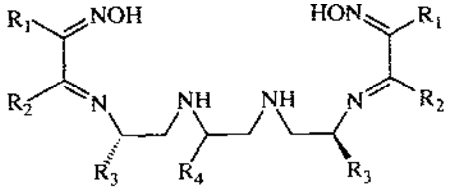

$R_1R_2L(1)H_2$ $R_3 = H, R_4 = H$

$R_1R_2L(2)H_2$ $R_3 = CH_3, R_4 = H$

$R_1R_2L(3)H_2$ $R_3 = CH_2Ph, R_4 = H$

$R_1R_2L(4)H_2$ $R_3 = H, R_4 = CH_3$

Fig. 8. The oxime–imine ligand, $R_1R_2L(1)H_2$, and its modified derivatives.

[74,75], $[\mathrm{Ni^{III/II}Me_2L(1)}]^{+/0}$ [74,75], $[\mathrm{Fe^{III/II}Me_2L(1)}]^{+/0}$ [74,76], and $[\mathrm{Co^{III}Me_2L(1)}]^{+}$ [77,78].

The nickel(IV) complexes have a distorted octahedral geometry [79] and show low substitution lability even in highly acidic media. They can also be optically resolved [80], and are good candidates for outer-sphere stereoselectivity studies. Problems of self-exchange racemization can be overcome with the use of chiral substituents on the ligand backbone which results [61,62] in the formation of a single diastereomer on complexation to the metal center, even in labile oxidation states (Fig. 9).

Stereoselectivity has been probed with the use of $[\mathrm{Co(edta)}]^{2-}$ as reductant and isolation of the inert $[\mathrm{Co(edta)}]^{-}$ product [61–63]. The mechanism for the reaction is

$$[\mathrm{Ni^{IV}Me_2L(1)}]^{2+}[\mathrm{Co(edta)}]^{2-} \rightarrow [\mathrm{Ni^{III}Me_2L(1)}]^{+} + [\mathrm{Co(edta)}]^{-} \qquad (15)$$

$$[\mathrm{Ni^{III}Me_2L(1)H}]^{2+} \rightleftharpoons [\mathrm{Ni^{III}Me_2L(1)}]^{+} + \mathrm{H}^{+} \qquad K_{\mathrm{H}} \qquad (16)$$

$$[\mathrm{Ni^{III}Me_2L(1)H}]^{2+} + [\mathrm{Co(edta)}]^{2-} \rightleftharpoons [\mathrm{Ni^{III}Me_2L(1)H^{2+}},[\mathrm{Co(edta)}]^{2-}] \qquad K_{\mathrm{ip}} \qquad (17)$$

$$[\mathrm{Ni^{III}Me_2L(1)H^{2+}},[\mathrm{Co(edta)}]^{2-}] \rightarrow [\mathrm{Ni^{II}Me_2L(1)H}]^{+} + [\mathrm{Co(edta)}]^{-} \qquad k_{\mathrm{et}} \qquad (18)$$

Biphasic kinetic behavior corresponds to the formation of the nickel(III) form as a transient intermediate, and stereoselectivity has been investigated in both steps. Initial results indicated [61,62] little difference in the stereoselectivities for the two steps despite differences in the details of the mechanisms but

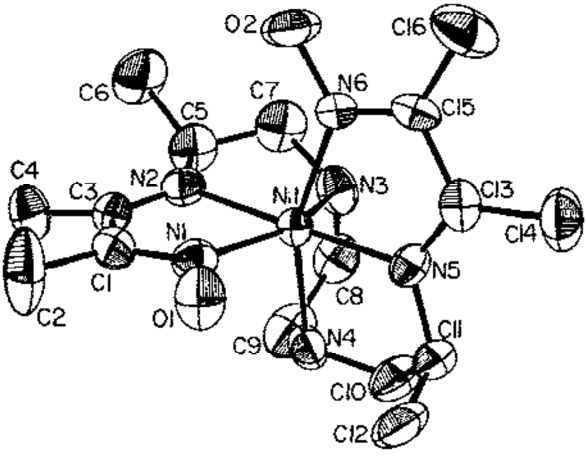

Fig. 9. Ortep of the $[\Lambda\text{-}\mathrm{Ni^{IV}Me_2L(2)}]^{2+}$ complex. (Reproduced with permission from ref. 62.)

subsequent studies [63] have shown this to be coincidental. Kinetics and stereoselectivity have also been investigated [81] in the oxidation of the corresponding iron(II) complex, $[Fe^{II}Me_2L(1)]$, by $[Co(edta)]^-$. Rate and stereoselectivity data for these reactions are presented in Table 5.

In efforts to understand the data, chiral recognition has been studied in the inert ion pair formed between $[Ni^{IV}Me_2L(1)]^{2+}$ and $[Co(edta)]^-$ [62]. No redox is possible and only the charge on $[Co(edta)]^-$ differs from the reaction pair. The experiment involves partial resolution of racemic $[Ni^{IV}Me_2L(1)]^{2+}$ by $[\Delta\text{-}Co(edta)]^-$ on a Sephadex ion-exchange column and reveals preferential formation of the ΔΛ diastereomer, mirroring chiral induction in the electron transfer process. Further information on the structure of the ion pair is derived from NMR studies [82] on the isostructural cobalt(III) complex, $[Co^{III}Me_2L(1)]^+$, where relaxation experiments with the paramagnetic relaxant $[Cr(edta)]^-$ indicate that the preferred ion pair involves a hydrogen bonded interaction between the amine hydrogen atom of the oxime-imine complex and a carboxylate oxygen of the $[Cr(edta)]^-$ (Fig. 10). This model for the precursor complex provides an important structural basis for interpretation of stereoselectivity.

Studies incorporating structural variations on the reactants are informative.

TABLE 5

Rate constants and stereoselectivities for reactions of bis(oxime–imine) complexes with $[Co(edta)]^{-/2-}$ at 25.0°C and 0.10 M ionic strength

Oxidant	Reductant	k_{so}[a] ($M^{-1}\ s^{-1}$)	e.e.[b] (%)	
$[\Lambda\text{-}Ni^{IV}Me_2L(2)]^{2+}$	$[Co(edta)]^{2-}$	33	10.8	ΔΛ
$[\Lambda\text{-}Ni^{IV}Me_2L(2)]^{2+}$	$[Co(pdta)]^{2-}$	48	10.7	ΔΛ
$[\Lambda\text{-}Ni^{IV}Me_2L(2)]^{2+}$	$[Co(cdta)]^{2-}$	45	11.4	ΔΛ
$[\Lambda\text{-}Ni^{IV}MePhL(2)]^{2+}$	$[Co(edta)]^{2-}$	122	20.8	ΔΛ
$[\Lambda\text{-}Ni^{IV}PhMeL(2)]^{2+}$	$[Co(edta)]^{2-}$	500	6.8	ΔΛ
$[\Lambda\text{-}Ni^{IV}Me_2L(3)]^{2+}$	$[Co(edta)]^{2-}$		22.5	ΔΛ
$[\Lambda\text{-}Ni^{IV}MePhL(3)]^{2+}$	$[Co(edta)]^{2-}$		46.4	ΔΛ[c]
$[\Lambda\text{-}Ni^{IV}Me_2L(4)]^{2+}$	$[Co(edta)]^{2-}$		3.5	ΔΛ
$[\Lambda\text{-}Ni^{III}Me_2L(2)H]^{2+}$	$[Co(edta)]^{2-}$	19	11.6	ΔΛ
$[\Lambda\text{-}Ni^{III}Me_2L(2)H]^{2+}$	$[Co(pdta)]^{2-}$	22	10.6	ΔΛ
$[\Lambda\text{-}Ni^{III}Me_2L(2)H]^{2+}$	$[Co(cdta)]^{2-}$	20	11.7	ΔΛ
$[\Lambda\text{-}Ni^{III}Me_2L(4)H]^{2+}$	$[Co(edta)]^{2-}$		8.5	ΔΛ
$[\Lambda\text{-}Fe^{III}Me_2L(2)OH]$	$[Co(edta)]^{2-}$		2	ΛΛ
$[Co(edta)]^-$	$[\Lambda\text{-}Fe^{II}Me_2L(2)]$	87	2	ΔΛ
$[Co(edta)]^-$	$[\Lambda\text{-}Fe^{II}Me_2L(2)H]^+$	≤0.6	11	ΔΛ

[a] Kinetic data for complexes with ligand $R_1R_2L(1)$.

[b] 23°C.

[c] 0.01 M ionic strength.

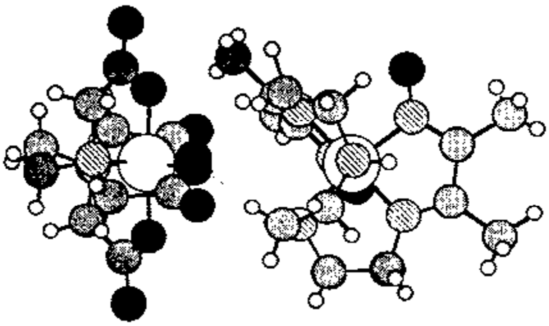

Fig. 10. Molecular model representing the structure of the precursor assembly formed between $[\mathrm{Ni^{IV}Me_2L(1)}]^{2+}$ and $[\mathrm{Co(edta)}]^{-}$ as determined by ^{1}H NMR T_1 relaxation experiments. The hydrogen bonding interaction is shown by the dotted line. (Reproduced with permission from ref. 82.)

There is little effect on either the stereoselectivity or the rate parameters when $[\mathrm{Co(pdta)}]^{2-}$ and $[\mathrm{Co(cdta)}]^{2-}$ are used instead of $[\mathrm{Co(edta)}]^{2-}$ as the reductants. Two deductions can be made from this observation. The origin of the stereoselectivity is not the result of a Pfeiffer effect since the $[\mathrm{Co(pdta)}]^{2-}$ and $[\mathrm{Co(cdta)}]^{2-}$ complexes do not racemize within the time scale of the electron transfer experiment. The second point is that it establishes the importance of the carboxylate face of the reductants for approach to the nickel oxidants, consistent with the picture which emerges from the ion-pairing interaction. Stereoselectivity in the oxidation of $[\mathrm{Co(edta)}]^{2-}$ by the series $[\Lambda\text{-}\mathrm{Ni^{IV}Me_2L(2)}]^{2+}$,$[\Lambda\text{-}\mathrm{Ni^{IV}PhMeL(2)}]^{2+}$ and $[\Lambda\text{-}\mathrm{Ni^{IV}MePhL(2)}]^{2+}$ reveals a greater effect when the bulky phenyl substituent is closest to the site of interaction with the reductant. Similar comments can be made about $[\Lambda\text{-}\mathrm{Ni^{IV}Me_2L(3)}]^{2+}$ and $[\Lambda\text{-}\mathrm{Ni^{IV}MePhL(3)}]^{2+}$ where the stereoselectivity reveals significant discrimination with $k_{\Delta\Lambda}/k_{\Delta\Delta}=2.7$. The structural variation is consistent with changes in chirality at the site of interaction between the complexes in the precursor ion pair rather than a balance of contributions from pathways of differing stereoselectivity as suggested previously [63]. For similarly charged reaction pairs, changes in the nature of the metal center have little effect on the extent and nature of the chiral induction [62,81], again consistent with a picture of a dominant role for the precursor ion pair structure.

Oxidation of $[\mathrm{Co(phen)_3}]^{2+}$ by $[\Lambda\text{-}\mathrm{Ni^{IV}Me_2L(2)}]^{2+}$ has also been examined [83,84]. Although the reaction also shows biphasic behavior, chiral induction for the individual steps cannot be determined. Instead, a combined value for reactions of both $[\Lambda\text{-}\mathrm{Ni^{IV}Me_2L(2)}]^{2+}$ and $[\Lambda\text{-}\mathrm{Ni^{III}Me_2L(2)H}]^{2+}$ is recorded (Table 6). The stereoselectivities are large, indicating strong interactions despite electrostatic repulsions due to the like charges.

The nature of the stereoselectivities is dependent on the oxidant structure

TABLE 6

Rate constants and stereoselectivities for reactions of bis(oxime–imine) complexes with $[Co(phen)_3]^{2+}$ at 25.0°C and 0.10 M ionic strength

Oxidant	Reductant	k_{so}[a] ($M^{-1}\ s^{-1}$)	e.e[b] (%)	
$[\Lambda\text{-}Ni^{IV}Me_2L(2)]^{2+}$	$[Co(phen)_3]^{2+}$	3.2×10^5	17	ΛΛ
$[\Lambda\text{-}Ni^{IV}MePhL(2)]^{2+}$	$[Co(phen)_3]^{2+}$	3.5×10^6	25	ΛΛ
$[\Lambda\text{-}Ni^{IV}PhMeL(2)]^{2+}$	$[Co(phen)_3]^{2+}$	3.0×10^7	9	ΛΔ
$[\Lambda\text{-}Ni^{IV}Me_2L(3)]^{2+}$	$[Co(phen)_3]^{2+}$	4.0×10^{6}[c]	36	ΛΛ
$[\Lambda\text{-}Ni^{IV}Me_2L(2)]^{2+}$	$[Co(bpy)_3]^{2+}$	6.5×10^5	3.5	ΛΛ
$[\Lambda\text{-}Fe^{III}Me_2L(2)H]^{2+}$	$[Co(phen)_3]^{2+}$	1.1×10^5	4	ΛΛ

[a] Kinetic data for complexes with ligand $R_1R_2L(1)$.

[b] Combined data for nickel(IV) and nickel(III) reduction, 23°C.

[c] Kinetic data for $[\Lambda\text{-}Ni^{IV}Me_2L(3)]^{2+}$.

and on electronic configuration. NMR relaxation experiments reveal [82] that the model interaction between $[Co^{III}Me_2L(1)]^+$ and $[Cr(phen)_3]^{3+}$ has no detectable structure and it is proposed that, for this series of reactions, electronic effects rather than precursor structure are dominant. The interesting switch in the sense of the induction from ΛΛ to ΔΛ for the $[Ni^{IV}PhMeL(2)]^{2+}$ reaction may be an exception as a stacking interaction between a phenanthroline ring of the reductant and the phenyl substituents in the oxidant is possible.

E. REACTIONS INVOLVING STRONG HYDROGEN BONDING

(i) Oxidation of $[Co(en)_3]^{2+}$ by $[Co(edta)]^-$ and related reactions

In a number of early studies [85–94], it was recognized that addition of 1,2-diaminoethane (en) to optically active solutions of derivatives of $[Co(edta)]^-$ resulted in chiral induction in the $[Co(en)_3]^{3+}$ formed. The results are summarized in Table 7. Attempts to explain the phenomenon in terms of stereoselective substitution processes are well documented but are confounded by the rapidity of the process, unusual for substitution reactions involving cobalt(III).

Geselowitz and Taube [35,95] provided an alternative explanation in terms of electron transfer catalysis by cobalt(II), and examined stereoselectivity in the stoichiometric electron transfer between $[Co(edta)]^-$ and $[Co(en)_3]^{2+}$ (eqn. (19)). The inert nature of both cobalt(III) complexes and the low rates of electron self-exchange between cobalt(II) and cobalt(III) greatly facilitate the examination of stereoselectivity and Geselowitz and Taube reported that

TABLE 7

Electron transfer catalyzed substitution reactions of $[Co(edta)]^-$ and derivatives

Reactant	Conditions	Product	e.e. (%)	Ref.
$[Co(edta)]^-$	50% en, 30°C	$[Co(en)_3]^{3+}$	26 ΔΛ	85
$[Co(edta)]^-$	50% en, 25°C	$[Co(en)_3]^{3+}$	13 ΔΛ	93
$[Co(edta)]^-$	anhyd. en, 25°C	$[Co(en)_3]^{3+}$	26 ΔΛ	93
$[Co(edta)]^-$	50% en, 44°C	$[Co(en)_3]^{3+}$	13.2 ΔΛ	87
$[Co(edta)]^-$	anhyd. en, 44°C	$[Co(en)_3]^{3+}$	26 ΔΛ	87
$[Co(edta)]^-$	10% pn, 50°C	$[Co(pn)_3]^{3+}$	83 ΛΛ	89
$[Co(edta)Cl]^{2-}$	50% en, 25°C	$[Co(en)_3]^{3+}$	9.6 ΔΛ	93
$[Co(edta)Cl]^{2-}$	anhyd. en, 25°C	$[Co(en)_3]^{3+}$	17 ΔΛ	93
$[Co(R\text{-}pdta)]^-$	~30% en, 25°C	$[Co(en)_3]^{3+}$	97 ΛΛ	90
$[Co(R\text{-}pdta)]^-$	50% en, 25°C	$[Co(en)_3]^{3+}$	~100 ΛΛ	86, 88
$[Co(R\text{-}pdta)]^-$	anhyd. en, 25°C	$[Co(en)_3]^{3+}$	34 ΔΛ	94
$[Co(R\text{-}pdta)]^-$	~10% pn, 25°C	$[Co(pn)_3]^{3+}$	100 ΛΛ	89
$[Co(trdta)]^-$	50% en, 25°C	$[Co(en)_3]^{3+}$	12 ΔΛ	90

the $[Co(en)_3]^{3+}$ formed shows an excess of 10% of the Λ isomer when the oxidant is $[\Delta\text{-}Co(edta)]^-$, indicating a preferred ΔΛ interaction. The stereoselectivity is modest but nevertheless, the system has become a prototype for a series of related studies.

$$[Co(edta)]^- + [Co(en)_3]^{2+} \rightarrow [Co(edta)]^{2-} + [Co(en)_3]^{3+} \tag{19}$$

The kinetics and mechanisms of the reduction of $[Co(edta)]^-$ and its derivatives by $[Co(en)_3]^{2+}$ and $[Co(sep)]^{2+}$ and $[Co(9aneN_3)_2]^{2+}$ have now been reported [58,59,96]. Rate data are presented in Table 8. The reactions are rapid and there are no detectable intermediates, suggesting that outer-

TABLE 8

Rate constants for reduction of $[Co(edta)]^-$ by $[Co(en)_3]^{2+}$ and derivatives

Oxidant	Reductant	Medium (M, °C)	k_{12} ($M^{-1}\,s^{-1}$)	Ref.
$[Co(edta)]^-$	$[Co(en)_3]^{2+}$	1.00, 25.0	5.24	59
$[Co(edta)]^-$	$[Co(en)_3]^{2+}$	0.14, 30.0	17	35
$[Co(pdta)]^-$	$[Co(en)_3]^{2+}$	1.00, 25.0	5.25	59
$[Co(cdta)]^-$	$[Co(en)_3]^{2+}$	1.00, 25.0	5.00	59
$[Co(edta)]^-$	$[Co(sep)]^{2+}$	0.10, 25.0	6×10^4	58
$[Co(edta)]^-$	$[Co(sep)]^{2+}$	0.10, 25.0	8.26×10^4	96
$[Co(edta)]^-$	$[Co(9aneN_3)_2]^{2+}$	0.10, 25.0	2.76×10^4	96
$[Co(cdta)]^-$	$[Co(sep)]^{2+}$	0.10, 25.0	8.30×10^4	96
$[Co(cdta)]^-$	$[Co(9aneN_3)_2]^{2+}$	0.10, 25.0	3.00×10^4	96

sphere mechanisms are operating in all cases [97]. Marcus calculations based on the best available estimates for the self-exchange rates for the reagents indicate that the rates are somewhat higher than expected, and a likely explanation is that the precursor for the cross-reaction is greatly stabilized by hydrogen bonding.

To gain more insight into the specific nature of this interaction, the effects of modification of reductant and oxidant structure on the overall stereoselectivity of the reaction have been reported. Variations in oxidant amine backbone structure [59], with use of the $[Co(edta)]^-$ derivatives $[Co(pdta)]^-$ and $[Co(cdta)]^-$, have minimal effect on the kinetics and stereoselectivity of the reaction, implying that it is the pseudo-C_3 carboxylate face of the complex which is involved in the stereoselective interaction. The effect of changes in the ligand structure of the reductant is more marked [58], and there are two important trends. The first is that stereoselectivity is very dependent on chelate ring conformation, with a trend from ΛΛ to ΔΛ as the number of *ob* conformations increases. The second is that, within a single conformation, stereoselectivity shows significant steric effects. For the lel_3 complexes, the stereoselectivity ranges from 25% ΔΔ with $[Co((\pm)\text{-chxn})_3\text{-}lel_3]^{2+}$ where the steric bulk of the ligand is in the C_2 plane of the complex to 17% ΔΛ for $[Co(sep)]^{2+}$ where the steric bulk is along the C_3 axis. These data are summarized in Table 9 and Fig. 11.

One factor which has facilitated an understanding of these studies is the

TABLE 9

Stereoselectivity in the reduction of $[Co(edta)]^-$ by $[Co(en)_3]^{2+}$ and derivatives

Oxidant	Reductant	Medium (M)	Stereoselectivity	Ref.
$[Co(edta)]^-$	$[Co(en)_3]^{2+}$	1.0	9.2% ΔΛ	35
$[Co(edta)]^-$	$[Co(en)_3]^{2+}$	0.057	11.5% ΔΛ	58
$[Co(edta)]^-$	$[Co(en)_3]^{2+}$	0.04	9.0% ΔΛ	59
$[Co(pdta)]^-$	$[Co(en)_3]^{2+}$	0.04	8.0% ΔΛ	59
$[Co(cdta)]$	$[Co(en)_3]^{2+}$	0.04	7.9% ΔΛ	59
$[Co(edta)]^-$	$[Co(sen)]^{2+}$	0.057	10.0% ΔΛ	58
$[Co(edta)]^-$	$[Co(sep)]^{2+}$	0.10	16.5% ΔΛ	58
$[Co(edta)]^-$	$[Co((\pm)\text{-bn})_3\text{-}lel_3]^{2+}$	0.052	14.2% ΔΔ	58
$[Co(edta)]$	$[Co((\pm)\text{-bn})_3\text{-}lel_2ob]^{2+}$	0.052	0.2% ΔΛ	58
$[Co(edta)]^-$	$[Co((\pm)\text{-bn})_3\text{-}lelob_2]^{2+}$	0.052	12.5% ΔΛ	58
$[Co(edta)]^-$	$[Co((\pm)\text{-bn})_3\text{-}ob_3]^{2+}$	0.052	25% ΔΛ	58
$[Co(edta)]^-$	$[Co((\pm)\text{-chxn})_3\text{-}lel_3]^{2+}$	0.052	24% ΔΔ	58
$[Co(edta)]^-$	$[Co((\pm)\text{-chxn})_3\text{-}lel_2ob]^{2+}$	0.052	5% ΔΔ	58
$[Co(edta)]^-$	$[Co((\pm)\text{-chxn})_3\text{-}lelob_2]^{2+}$	0.052	7% ΔΛ	58
$[Co(edta)]^-$	$[Co((\pm)\text{-chxn})_3\text{-}ob_3]^{2+}$	0.052	16% ΔΛ	58

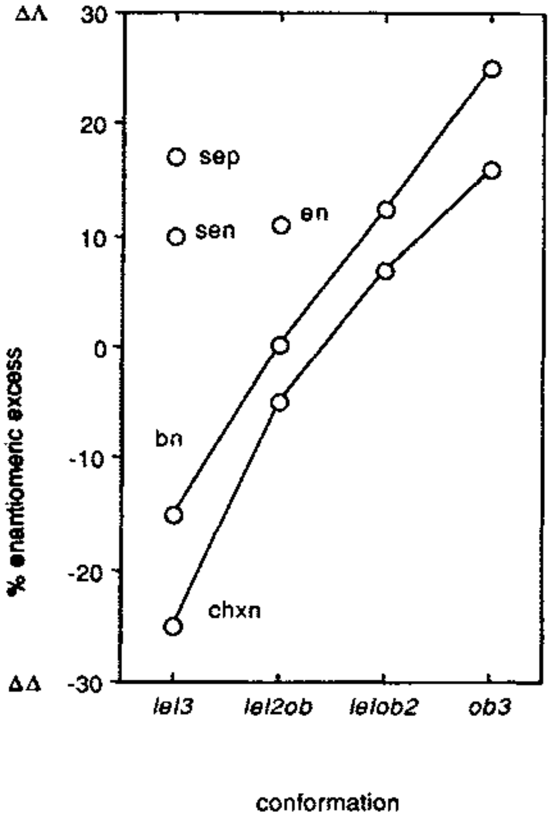

Fig. 11. Plot of stereoselectivity against reductant chelate ring conformation for the reaction between $[Co(edta)]^-$ and cobalt(II) amine reductants.

availability of ion-pairing stereoselectivities for a number of inert isostructural analogs which differ only in their charges from the redox active species (Table 10) [60,98–101]. There is a close qualitative relationship between ion-pairing and electron transfer stereoselectivities which has led to the proposal

TABLE 10

Comparison of stereoselectivity in electron transfer and ion-pair formation

		Stereoselectivity		Ref.
		IP	ET	
$[Co(edta)]^-$	$[Co(en)_3]^{3+}$	ΔΛ	ΔΛ	58, 98
$[Co(edta)]^-$	$[Co(sep)]^{3+}$	ΔΛ	ΔΛ	58, 98
$[Co(edta)]^-$	$[Co((\pm)\text{-chxn})_3\text{-}lel_3]^{3+}$	ΔΔ	ΔΔ	58, 98

[58] that, in this system, precursor ion-pair structure may play a dominant role in determining the electron transfer stereoselectivity. Chiral induction can thus be discussed in terms of chiral discrimination in precursor ion-pair structure rather than in terms of a more complex electronic effect.

Yoneda and coworkers [98,99] have explained ion pairing stereoselectivity on the basis of the differing helicities described by the C_2 and C_3 axes of a tris-chelate complex ion (Fig. 2). For a Δ isomer, this is designated as $P(C_3)M(C_2)$ and for a Λ isomer as $M(C_3)P(C_2)$. Since the C_3 axis in $[Co(sep)]^{3+}$ is blocked, chiral discrimination in this complex is likely to be dominated by interactions along the C_2 axis. Similarly, for $[Co((\pm)\text{-chxn})_3\text{-}\mathit{lel}_3]^{3+}$, discrimination is likely to arise from interactions along the C_3 axis. These two complexes show preferential interactions with different enantiomers of $[Co(edta)]^-$ which is reasoned to use its pseudo-C_3 carboxylate face in interactions with all the cations. Thus, the helicity described along the axis of approach of $[Co(edta)]^-$ to the reductant dominates the stereoselectivity.

While steric hindrance controls the preferred orientation of the oxidant within a single conformation, it does not provide a satisfactory explanation for the effect of changing chelate ring conformation. Some understanding of the effects of chelate ring conformation can be helpful in evaluating the types of interactions involved. When a five-membered chelate ring in $[Co(en)_3]^{3+}$ changes from a *lel* to an *ob* conformation, the configuration of the amine protons changes from parallel to the C_3 axis of the complex where it is oriented for a strong linear hydrogen bond along this axis, to a position which is oblique to the axis (Fig. 12). Changes in stereoselectivity due to

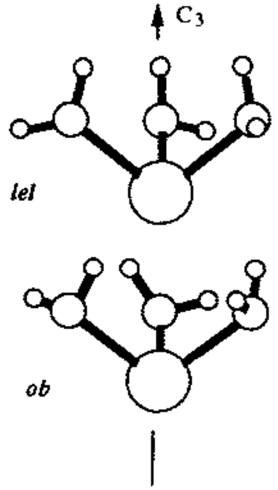

Fig. 12. Representations of the amine hydrogen atom configurations for the *lel* and *ob* conformations of the 1,2-diaminoethane (en) ligands in the $[Co(en)_3]^{3+}$ complex.

changes in chelate ring conformation can therefore be interpreted in terms of hydrogen-bonding interactions along the C_3 axis, and this linear dependence observed with $[Co(edta)]^-$ is a characteristic of strong hydrogen bonding. Clearly, in this case, directional factors such as hydrogen bonding are more important than shape selectivity. Detailed schematics of the ion-pair precursors based on the above stereoselectivity results are presented in Fig. 13. The modest stereoselectivities observed in the electron transfer reactions result from the multiplicity of available interactions.

Information on the nature of the ion-pair formed between $[Co(edta)]^-$ and $[Co(en)_3]^{3+}$ comes from a variety of sources. Recent NMR investigations [102] of the effect of addition of $[Cr(en)_3]^{3+}$ on the ^1H relaxation rates of $[Co(edta)]^-$ are consistent with a model in which the carboxylate face of the $[Co(edta)]^-$ is presented to the paramagnetic cation (Fig. 14), but the high symmetry of the $[Co(en)_3]^{3+}$ ion precludes any details on the cationic complex orientation. These conclusions for the preferred mode of interaction agree with the stereoselectivity results. A more general discussion of the role of the precursor in determining stereoselectivity is to be found in Sect. E. (iii).

Geselowitz et al. [59] investigated the effect of changing solvent on stereoselectivity in the oxidation of $[Co(en)_3]^{2+}$ by $[Co(edta)]^-$ (Table 11), and found enhancement, particularly in dipolar aprotic solvents. It was proposed that the lower stereoselectivity detected in protic media might be an indication

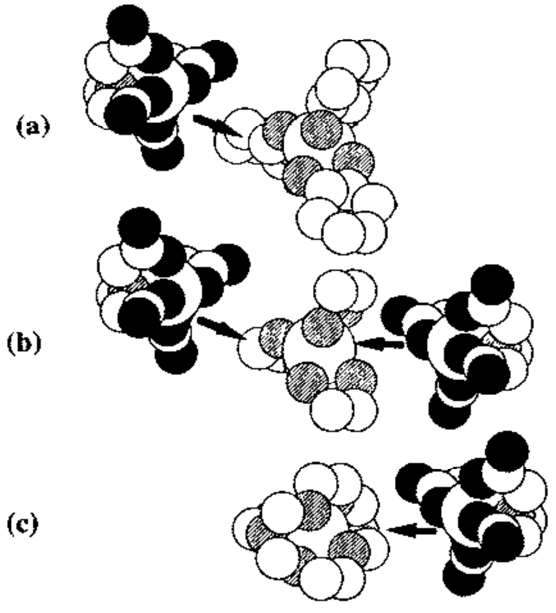

Fig. 13. Space-filling representations of the preferential interactions of $[Co(edta)]^-$ with cobalt(II) amine complexes: (a) $[Co((\pm)\text{-chxn})_3\text{-}\mathit{lel}_3]^{2-}$; (b) $[Co(en)_3\text{-}\mathit{lel}_3]^{2-}$; (c) $[Co(sep)\text{-}\mathit{lel}_3]^{2+}$ [58].

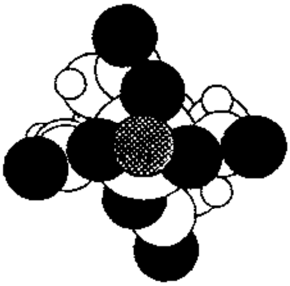

Fig. 14. View along the Cr–Co axis showing the calculated position of the paramagnetic center, $[Cr(en)_3]^{3+}$, cross-hatched, in the ion pair with $[Co(edta)]^-$. (Reproduced with permission from ref. 102.)

TABLE 11

Effect of solvent on the electron transfer stereoselectivity for the oxidation of $[Co(en)_3]^{2+}$ by $[Co(edta)]^-$ at 25.0°C

Solvent	e.e (%)	$k_{\Delta\Lambda}/k_{\Delta\Delta}$
H_2O	9.0	1.2
$(CH_2OH)_2$	13.0	1.3
$HCONH_2$	18.3	1.4
CH_3CH_2OH	17.4	1.4
CH_3OH	17.3	1.4
$HCON(CH_3)_2$	31.4	1.9
$(CH_3)_2SO$	34.5	2.0
$(CH_2)_4SO$	44.9	2.3

that hydrogen bonding with the solvent disrupts the interactions between the ions. However, an increase in ΔΛ stereoselectivity may also be caused by an increase in the *ob* character of the chelate ring conformation.

Vibrational circular dichroism studies indicate [103] that the *lel*$_3$ conformation dominates in DMSO solution while the *lel*$_2$*ob* conformation predominates in water. Experiments conducted with $[Co((\pm)\text{-chxn})_3]^{2+}$ as reductant have been used to elucidate this phenomenon with some surprising results [104]. There is indeed the expected increase in the proportion of *lel*$_3$ conformer, enhanced in the presence of chloride ion, but stereoselectivity found for $[Co((\pm)\text{-chxn})_3\text{-}lel_3]^{3+}$ is 50% ΔΛ in DMSO compared with 24% ΔΔ in water. Furthermore, the strong trend in stereoselectivity with a changing chelate ring conformation observed in aqueous media is absent (Table 12). Clearly, there are substantial differences in the mode of interaction between the complexes depending on the solvent.

TABLE 12

Electron transfer stereoselectivity in the oxidation of $[Co((\pm)\text{-chxn})_3]^{2+}$ by $[\Delta\text{-Co(edta)}]^-$ in DMSO and H_2O at 23°C

	DMSO	DMSO (0.6 M Cl^-)	H_2O
lel_3	50% Λ	43% Λ	24% Δ
lel_2ob	72% Λ	58% Λ	5% Δ
$lelob_2$	76% Λ		7% Λ
ob_3	59% Λ		16% Λ

(ii) Oxidation of $[Co(en)_3]^{2+}$ by $[Co(ox)_3]^{3-}$, $[Co(mal)_3]^{3-}$

The oxidants $[Co(ox)_3]^{3-}$ and $[Co(mal)_3]^{3-}$ possess C_3 carboxylate faces similar to the pseudo-C_3 face of $[Co(edta)]^-$ and have been employed in kinetic and stereoselectivity studies with $[Co(en)_3]^{2+}$ and derivatives [60,105]. In the case of $[Co(ox)_3]^{3-}$, the mechanism is described by competing inner-sphere and outer-sphere pathways (eqns. (20)–(22)) with rate constants $k_i = 3300\ M^{-1}\ s^{-1}$ and $k_o = 390\ M^{-1}\ s^{-1}$, respectively.

$$[Co(en)_2]^{2+} + en \rightleftharpoons [Co(en)_3]^{2+} \qquad K_3 = 2000\ M^{-1} \tag{20}$$

$$[Co(en)_2]^{2+} + [Co(ox)_3]^{3-} \rightarrow [Co(en)_2(ox)]^+ + [Co(ox)_2]^{2-} \qquad k_i \tag{21}$$

$$[Co(en)_3]^{2+} + [Co(ox)_3]^{3-} \rightarrow [Co(en)_3]^{3+} + \text{“}[Co(ox)_3]^{4-}\text{”} \qquad k_o \tag{22}$$

When optically active $[Co(ox)_3]^{3-}$ is used, both pathways show chiral induction. Inner-sphere stereoselectivity is small, 1.5% ΔΔ, while the outer-sphere value, 8% ΔΛ, is comparable with that observed with $[Co(edta)]^-$. The inner-sphere stereoselectivity is discussed in further detail in Sect. I.

The outer-sphere pathway between $[Co(ox)_3]^{3-}$ and $[Co(en)_3]^{2+}$ has a ΔΛ stereoselectivity. It has not proved possible to model chiral recognition in the precursor by examining the interaction between $[Co(ox)_3]^{3-}$ and $[Co(en)_3]^{3+}$, but selective crystallization shows a ΔΛ preference which parallels chiral induction in the reaction [106]. Outer-sphere stereoselectivities have been determined with a range of reductants and are presented in Table 13. There is generally good agreement with the corresponding values for reactions of $[Co(edta)]^-$ except that the trend with chelate ring conformation for both $[Co((\pm)\text{-chxn})_3]^{2+}$ and $[Co((\pm)\text{-bn})_3]^{2+}$ is less well defined for $[Co(ox)_3]^{3-}$ than for $[Co(edta)]^-$, and the ordering for $[Co((\pm)\text{-chxn})_3\text{-}lel_3]^{2+}$ is out of sequence. In fact this parallels the behavior shown by $[Co(edta)]^-$ in DMSO (Fig. 15). Studies with $[Co(ox)_3]^{3-}$ in DMSO are similar to values in aqueous solution, suggesting that this behavior represents

TABLE 13

Stereoselectivity in the reduction of $[Co(edta)]^-$, $[Co(ox)_3]^{3-}$ and $[Co(mal)_3]^{3-}$ by $[Co(en)_3]^{2+}$ and derivatives

Reductant	Stereoselectivity		
	$[Co(edta)]^-$	$[Co(ox)_3]^{3-}$	$[Co(mal)_3]^{3-}$
$[Co(en)_3]^{2+}$	11.5% ΔΛ	7.6% ΔΛ	0.6% ΔΛ
$[Co(sen)]^{2+}$	9.8% ΔΛ	6.6% ΔΛ	
$[Co(sep)]^{2+}$	17.6% ΔΛ	>21% ΔΛ	
$[Co((\pm)\text{-bn})_3\text{-}lel_3]^{2+}$	14.2% ΔΔ	28% ΔΔ	
$[Co((\pm)\text{-bn})_3\text{-}lel_2ob]^{2+}$	0.15% ΔΛ	14% ΔΔ	
$[Co((\pm)\text{-bn})_3\text{-}lelob_2]^{2+}$	12.5% ΔΛ	9% ΔΔ	
$[Co((\pm)\text{-bn})_3\text{-}ob_3]^{2+}$	25% ΔΛ	14% ΔΔ	
$[Co((\pm)\text{-chxn})_3\text{-}lel_3]^{2+}$	24% ΔΔ	38% ΔΛ	23% ΔΔ
$[Co((\pm)\text{-chxn})_3\text{-}lel_2ob]^{2+}$	5% ΔΔ	56% ΔΛ	26% ΔΔ
$[Co((\pm)\text{-chxn})_3\text{-}lelob_2]^{2+}$	7% ΔΛ	68% ΔΛ	24% ΔΔ
$[Co((\pm)\text{-chxn})_3\text{-}ob_3]^{2+}$	16% ΔΛ	51% ΔΛ	15% ΔΔ

a limiting condition in which intimate electrostatic interactions dominate over hydrogen bonding forces. The reagent $[Co((\pm)\text{-chxn})_3]^{2+}$ is particularly useful for the discussion of stereoselectivity in these reactions because steric constraints restrict approach of the oxidant to the C_3 axis.

Studies with $[Co(mal)_3]^{3-}$ reveal an entirely different picture. Stereoselectivity with $[Co(en)_3]^{2+}$ is very small, 0.6% ΔΛ [60,105]. With the conformationally restricted $[Co((\pm)\text{-chxn})_3]^{2+}$ there is little dependence on the chelate ring conformation. The $[Co(mal)_3]^{3-}$ complex differs from $[Co(ox)_3]^{3-}$ in having steric hindrance along the C_3 axis from terminal carboxylate oxygens. Hydrogen-bonding forces are, therefore, favored over more intimate electrostatic interactions. Interestingly, preliminary results [60] for this oxidant with $[Co((\pm)\text{-pn}_3]^{2+}$ shown an enhanced stereoselectivity and attention should be called to the X-ray structure of the $[\Delta\text{-}Co((-)\text{-pn})_3][\Delta\text{-}Cr(mal)_3]\cdot 3H_2O$ in which an extended network of hydrogen-bonding dominates the stereospecific interaction (Fig. 16) [107].

Stereoselectivity studies with a number of other oxidants have also been reported although no complimentary kinetic data are available. When comparisons with isostructural analogs have been possible in these strongly hydrogen-bonded systems [58,60,62], there is good though not complete agreement between ion-pair and electron transfer stereoselectivities (Table 14). The exceptions to this general rule of thumb clearly weaken the case for a dominant ion-pair interaction in the determination of stereoselectivity and necessitate consideration of stereoelectronic factors. A number of calculations have been carried out in systems where both electrostatic and hydrogen

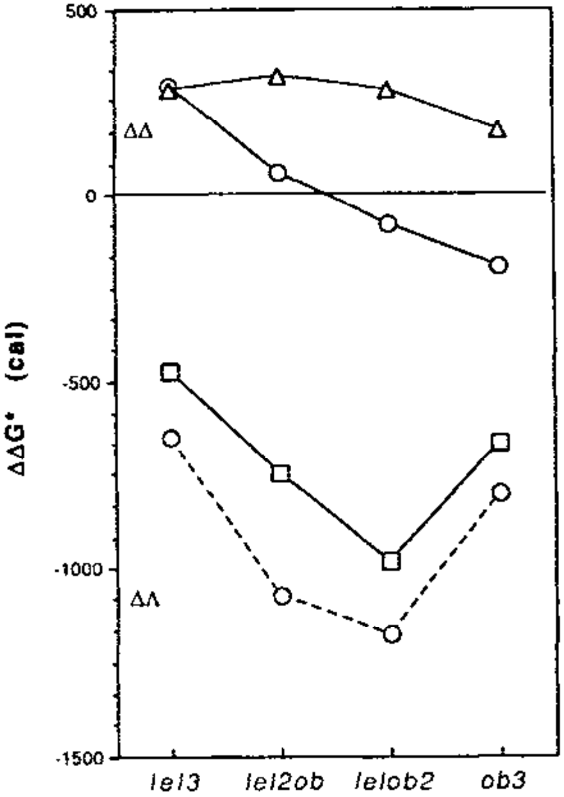

Fig. 15. Stereoselectivity shown as $\Delta\Delta G^*$ ($\Delta G^*_{\Delta\Delta} - \Delta G^*_{\Delta\Lambda}$) in the reactions of $[Co(edta)]^-$ (○) and $[Co(ox)_3]^{3-}$ (□) with $[Co((\pm)\text{-chxn})_3]^{2+}$ in water (——) and DMSO (----) as a function of chelate ring conformation.

bonding forces are included and they reveal that electronic factors dominate the stereoselectivity by a factor of around five [58]. The bulk of this electronic effect can be traced to solvation changes in attaining the electron transfer transition state. However, the calculations involve a variety of questionable assumptions and have little predictive power.

It should be noted in Table 14 that all the systems which give an opposing correspondence between ion-pairing and electron transfer stereoselectivities involve systems where the anion does not have a well defined C_3 or pseudo-C_3 axis. Further, in those instances, the stereoselectivities are very small. It may well be that the presence of a C_3 carboxylate face not only provides a chiral feature where negative charge and the oxygen lone pairs essential for hydrogen bonding are concentrated, but also the shortest distance between the metal center and the periphery of the molecule, important for orbital overlap and electron transfer. In the absence of this feature, the most stable ion-pair may well be a dead-end complex. Thus, at the risk of introducing a

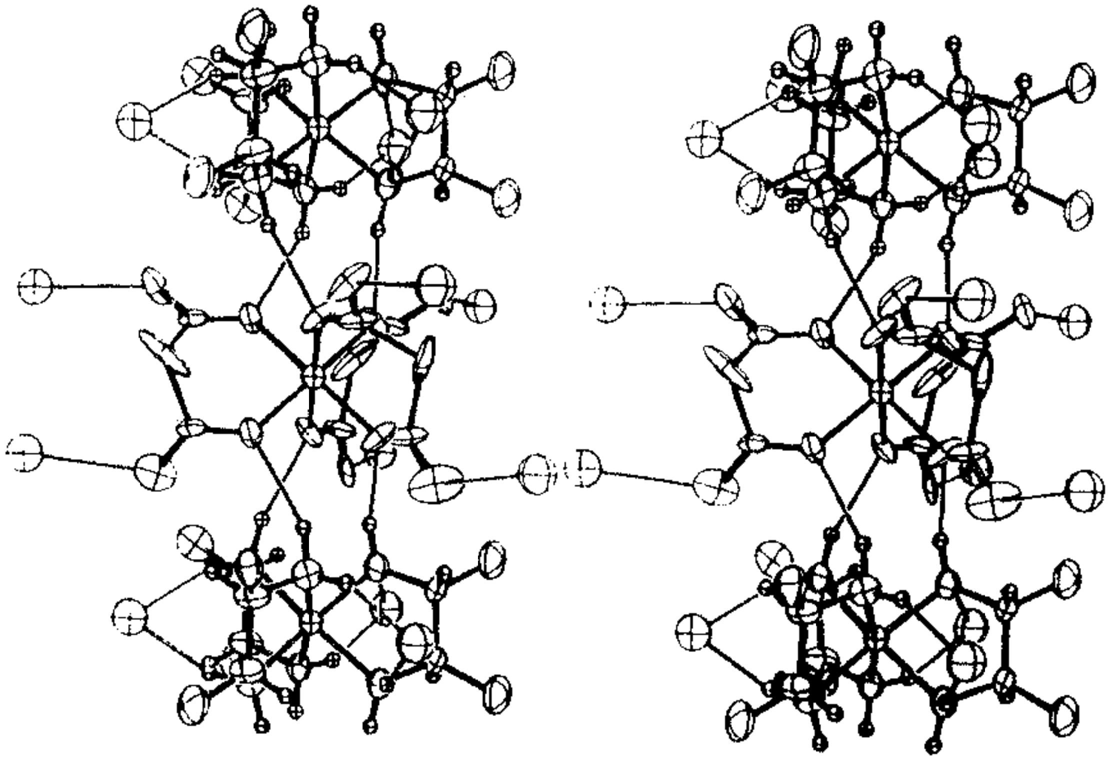

Fig. 16. X-ray structure of the [Δ-Co((−)-pn)$_3$][Λ-Cr(mal)$_3$]·3 H_2O interaction. (Reproduced with permission from ref. 107.)

TABLE 14

Stereoselectivities in electron transfer reactions and ion-pair precursor models

Reactants	ET	IP
$[Co(ox)_3]^{3-} + [Co(en)_3]^{2+}$	10.1% ΔΛ	ΔΔ
$[Co(ox)_2(gly)]^{2-} + [Co(en)_3]^{2+}$	9.0% ΔΛ	ΔΛ
$[Co(ox)_2(en)]^{-} + [Co(en)_3]^{2+}$	3.6% ΔΛ	ΔΔ
$[Co(edta)]^{-} + [Co(en)_3]^{2+}$	9.7% ΔΛ	ΔΛ
cis(N)-$[Co(ida)_2]^{-} + [Co(en)_3]^{2+}$	9.2% ΔΛ	ΔΛ
C_1-*cis*(N)-$[Co(ox)(gly)_2]^{-} + [Co(en)_3]^{2+}$	9.4% ΔΛ	ΔΛ
C_2-*cis*(N)-$[Co(ox)(gly)_2]^{-} + [Co(en)_3]^{2+}$	2.1% ΔΛ	ΔΔ
trans(N)-$[Co(ox)(gly)_2]^{-} + [Co(en)_3]^{2+}$	0.5% ΔΛ	ΔΔ
$[Co(mal)_3]^{3-} + [Co(en)_3]^{2-}$	1% ΔΛ	ΔΛ

hint of dogma, where ion-pair and electron transfer stereoselectivities coincide, the most stable ion pair is an active precursor in the electron transfer process, but when the stereoselectivities differ, the ion-pair is a 'dead-end' species which does not actively participate in the electron transfer process.

(iii) Stereoselectivity in ion-pair formation

In the interpretation of electron transfer stereoselectivities in these strongly hydrogen-bonded systems, much has been made of the role of the precursor ion pair and of comparisons with isostructural analogs as models for the ion-pairing interaction. The information available for ion-pairing stereoselectivities is now quite extensive and while considerable confusion remains in interpreting the data, a brief survey of the area is both appropriate and informative.

The earliest work on stereoselective interactions between metal ion complexes concerned investigations [33,108–110] of the Pfeiffer effect and its use in the assignment of absolute configurations (Table 15). Most of these data have been considered previously but it is from attempts to understand the mechanisms involved in these interactions that much of the information about hydrogen-bonding systems is derived. Other methods have also been employed. For example, the rate of proton exchange [111] in [Λ-Co(edta)]$^{-}$ is enhanced in the presence of [Δ-$Co(en)_2(NO_2)_2]^{+}$ compared with [Λ-$Co(en)_2(NO_2)_2]^{+}$. However, recent conductivity experiments give no evidence that this is a thermodynamic effect [112].

Tatehata et al. [113] examined ion-pairing in the $[Co(en)_3]^{3+}$/$[Co(ox)_2gly]^{2-}$ system by conductivity and ion-exchange chromatography and showed that $K_{\Delta\Lambda}$ (482 M^{-1}) > $K_{\Delta\Delta}$ (456 M^{-1}) at 25.0°C and 0.01 M ionic strength. Only the C_1-*cis*(N)-$[Co(ox)(gly)_2]^{-}$ complex which has three carboxylate groups arranged around a pseudo-C_3 axis can be resolved com-

TABLE 15

Ion-pairing stereoselectivities determined by the Pfeiffer effect

Reactants		Stereoselectivity	Ref.
$[Co(phen)_3]^{3+}$	$[Co(acac)_3]^-$	ΔΛ	33
$[Co(phen)_3]^{3+}$	$[Co(ox)_3]^{3-}$	ΛΛ	109
$[Co(sep)]^{3+}$	$[Cr(ox)_2(acac)]^2$	ΔΛ	108
$[Co(sep)]^{3+}$	$[Cr(ox)_2(gly)]^{2-}$	ΔΛ	108
$[Co(en)_3]^{3+}$	$[Cr(ox)_2(acac)]^{2-}$	ΛΛ	108
$[Co(en)_3]^{3+}$	$[Cr(ox)_2(gly)]^{2-}$	ΔΛ	108
$[Co((+)\text{-}pn)_3]^{3+}$	$[Cr(ox)_2(acac)]^{2-}$	ΛΛ	108
$[Co((+)\text{-}pn)_3]^{3+}$	$[Cr(ox)_2(gly)]^{2-}$	ΛΛ	108
$[Co(phen)_3]^{3+}$	$[Cr(ox)_2(acac)]^{2-}$	ΛΛ	108
$[Co(phen)_3]^{3+}$	$[Cr(ox)_2(gly)]^{2-}$	ΛΛ	108
$[Co(en)_2(gly)]^{2+}$	$[Cr(ox)_3]^3$	ΔΛ	110
$[Co(en)_2(acac)]^{2+}$	$[Cr(ox)_3]^{3-}$	ΔΛ	110

pletely by chromatography with $[Co(en)_3]^{3+}$ as eluant, and on this basis, a model involving three hydrogen bonds along the C_3 axis of $[Co(en)_3]^{3+}$ is proposed.

Yoneda and coworkers [98,99] examined a more extensive range of ion-pairs by two chromatographic techniques and presented a rather different picture in which the overall molecular shape plays a dominant role. In particular, the differing helicities along the C_3 and C_2 axes of a tris-chelate complex provide a means of discrimination. Depending on the axis which dominates the interaction, the counter ion will experience either M or P helicity. Steric arguments provide a basis for deciding whether a complex will prefer a C_3 interaction ($C_3{}^+$), for example $[Co((\pm)\text{-}chxn)_3]^{3+}$, or a C_2 interaction ($C_2{}^+$), for example $[Co(sep)]^{3+}$, and help establish characteristic patterns (Table 16). The bulk of the data can be rationalized in terms of preferred PP or MM pairs. Thus, a cation which has a dominant C_3 interaction such as $[Co((\pm)\text{-}chxn)_3]^{3+}$ will give a ΔΔ stereoselectivity with a C_3 dominated anion such as $[Co(edta)]^-$ and a ΔΛ stereoselectivity with a C_2 dominated anion such as $[Co(ox)_2(en)]^-$. A comment is required about $[Co(en)_3]^{2+}$ where a dominant role for the C_2 axis is assigned even though both C_2 and C_3 interactions are sterically allowed. This is rationalized in terms of the fluxional behavior of the chelate rings and their effect on the axial C_3 hydrogen bonding interaction.

Any rationalization of the stereoselectivity data which does not take account of the dominant directional nature of hydrogen bonds is clearly unsatisfactory. Yoneda and coworkers have subsequently modified [100] their arguments based on patterns of hydrogen bonding between amine protons on the cationic complex and bound carboxylate oxygens on the anionic

TABLE 16

Classification and selected ion pair stereoselectivities according to refs. 98–100

	$[Co(en)_3]^{3+}$	$[Co(sen)]^{3+}$	$[Co(sep)]^{3+}$	$[Co(chxn)_3]^{3+}$	$[Co(pn)_3]^{3+}$
	$(C_2^+ + C_3^+)$		(C_2^+)	(C_3^+)	
$[Co(edta)]^-$	ΔΛ		ΔΛ	ΔΔ	
$[Co(tdta)]^-$	ΔΛ		ΔΛ	ΔΔ	
$[Co(ox)_2(en)]^-$ (C_2^-)	ΔΔ	ΔΛ	ΔΛ	ΔΔ	ΔΛ
$[Co(mal)_2(en)]^-$	ΔΔ		ΔΔ	ΔΛ	
$[Co(ox)_2(gly)]^{2-}$ $(C_2^- + C_3^-)$	ΔΛ	ΔΛ	ΔΛ	ΔΔ	ΔΔ
$[Cr(mal)_3]^{3-}$	ΔΛ		ΔΛ	ΔΔ	
fac-$[Co(\beta\text{-ala})_3]$	ΔΔ		ΔΛ	ΔΔ	
C_2-*cis*(N)-$[Co(ox)(gly)_2]^-$ (C_2^-)	ΔΔ	ΔΛ	ΔΛ	ΔΔ	ΔΛ
C_1-*cis*(N)-$[Co(ox)(gly)_2]^-$ (C_3^-)	ΔΛ	ΔΛ	ΔΛ	ΔΔ	ΔΔ

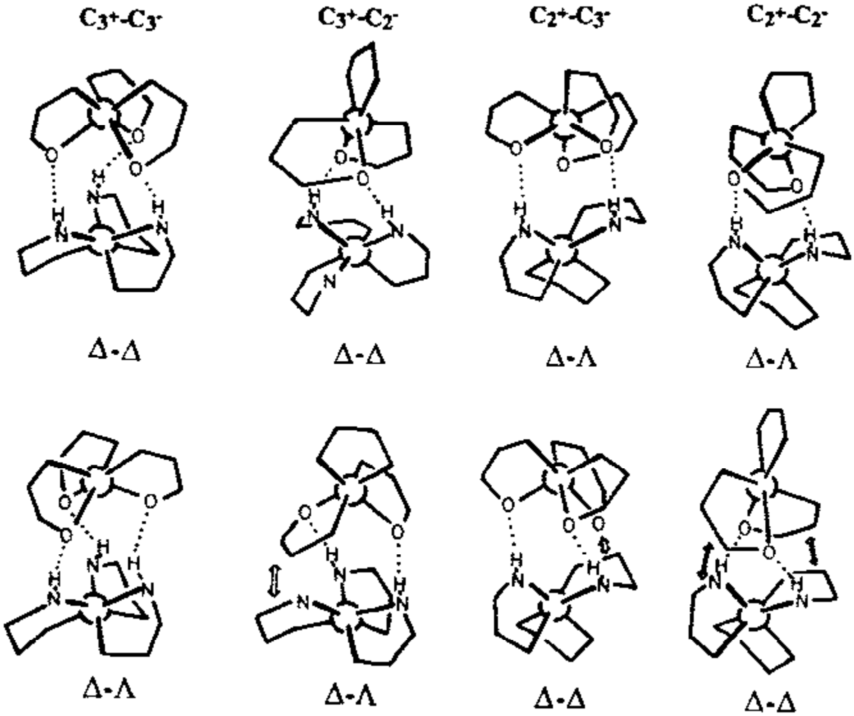

Fig. 17. Hydrogen bonding interactions for ion pairs involving a Δ cation complex and a Δ or Λ anion complex. Favorable pairs are shown in the upper part, unfavorable interactions are indicated by arrows. (Modified from ref. 100.)

complex along the C_3 and C_2 axes (Fig. 17). Again, the complexes are divided into groups depending on the axis of dominant interaction, and it is concluded that homochiral pairwise interactions (ΔΔ and ΛΛ) are favored for $C_3{}^+$ complexes and heterochiral pairwise interactions (ΔΛ and ΛΔ) for $C_2{}^+$ complexes, regardless of the axis preferred by the anion. Attention is again focussed on interactions of $[Co(en)_3]^{3+}$ which is classified as $(C_3{}^+ + C_2{}^+)$ with both axes unrestricted by steric hindrance. However, it is noted that, although $[Co(en)_3]^{3+}$ shows $C_3{}^+$ behavior, discrimination is much smaller than when it shows $C_2{}^+$ behavior, because of the fluxional nature of hydrogen-bonding interactions along the C_3 axis. Comparisons of results with $[Co(en)_2\mathit{N,N'}\text{-}Me_2en]^{3+}$, which has an additional steric interaction along the C_3 axis tend to support this view, but require that the C_3 interactions involve only two of the three possible hydrogen-bonds.

Tatehata and coworkers [114] have used chromatographic and conductivity measurements to examine interactions of $[Co(en)_3]^{3+}$ with a series of anionic complexes which have a pseudo-C_3 carboxylate face as a common structural feature (Table 17). In all cases, the stereoselectivity is ΔΛ. The

TABLE 17

Ion-pairing stereoselectivities at 25.0°C and 0.01 M ionic strength

Ion Pair	$K_{\Delta\Lambda}$	$K_{\Lambda\Lambda}$	$K_{\Delta\Lambda}/K_{\Lambda\Lambda}$	
$[Co(en)_3]^{3+}$,C_1-*cis*(N)-$[Co(ox)(gly)_2]^-$	83.1	63.8	1.31	ΔΛ
$[Co(en)_3]^{3+}$,β-*cis*(N)-$[Co(ox)(edda)]^-$	69.8	60.0	1.16	ΔΛ
$[Co(en)_3]^{3+}$,$[Co(edta)]^-$	125	119	1.06	ΔΛ
$[Co(en)_3]^{3+}$,*cis*(N)-$[Co(ida)_2]^-$	188	179	1.05	ΔΛ
$[Co(en)_3]^{3+}$,C_1-*cis*(N)-$[Co(ox)(\beta\text{-ala})_2]^-$				ΔΛ
$[Co(en)_3]^{3+}$,$[Co(ox)_2(gly)]^{2-}$	482	456	1.06	ΔΛ
$[Co(en)_3]^{3+}$,$[Co(ox)_2(ala)]^{2-}$				ΔΛ
$[Co(en)_3]^{3+}$,$[Co(mal)_2(gly)]^{2-}$				ΔΛ
$[Co(en)_3]^{3+}$,$[Co(mal)_2(ala)]^{2-}$				ΔΛ

discrimination mechanism proposed by this group involves a triple hydrogen bond between the amine hydrogens on the C_3 axis of $[Co(en)_3]^{3+}$ and the bound carboxylate oxygen atoms (Fig. 18), and is in disagreement with the proposals of Yoneda. However, it is supported by induced circular dichroism measurements [114]. An interesting feature is that, of the isomers of $[Co(ox)(gly)_2]^-$, effective discrimination takes place only with the C_1-*cis*(N) derivative, the only one with a pseudo-C_3 carboxylate face. The effect of changes in the orientation of the carboxylate oxygen lone pairs for hydrogen bonding is revealed in the discrimination order C_1-*cis*(N)-$[Co(ox)(\beta\text{-ala})_2]^- >$ C_1-*cis*(N)-$[Co(ox)(gly)_2]^- >$ β-*cis*(N)-$[Co(ox)(edda)]^-$.

The lack of any coherent picture from these data on chiral discrimination underscores the difficulties involved in interpreting chiral induction in electron transfer reactions. A factor which appears to be overlooked is that ion pair geometry is dynamic and that the dominant interactions may not provide the greatest discrimination. Information which might resolve these problems is only partially available. As noted previously [102], NMR relaxation experiments indicate that $[Co(edta)]^-$ uses its pseudo-C_3 face in interacting with $[Co(en)_3]^{3+}$ and there is an important crystal structure [107] for the $[\Delta\text{-}Co((-)\text{-}pn)_3\text{-}lel_3]^{3+}[\Delta\text{-}Cr(mal)_3]^{3-}$ system in which the complexes are arranged with three hydrogen bonds along mutual C_3 axes. However, it is pointed out that the stereoselective crystallization may not be the result of this hydrogen-bonding interaction. Interestingly, the results of simple calculations for the approach of the highly symmetric pair $[Co(en)_3]^{3+}$ and $[Co(ox)_3]^{3-}$ along different axes reveal that C_3C_3 interactions are favored over C_3C_2 interactions but that stereoselectivity for approach along the former direction is dependent on whether hydrogen bonding (ΔΛ) or van der Waal's repulsions (ΔΔ) dominate [115].

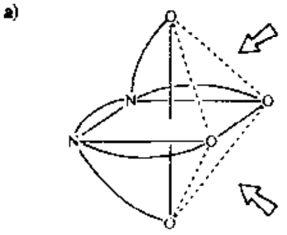

$[Co(edta)]^-$

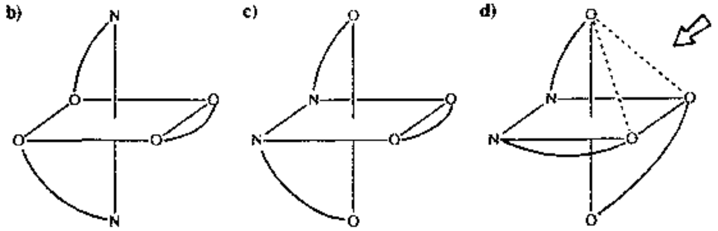

trans(N) C_2-cis(N) C_1-cis(N)

$[Co(ox)(gly)_2]^-$

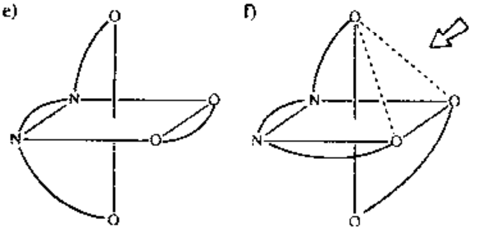

α-cis β-cis

$[Co(ox)(edda)]^-$

Fig. 18. Structures for the anionic complexes: (a) $[Co(edta)]^-$, (b)–(d) $[Co(ox)(gly)_2]^-$ and (e), (f) $[Co(ox)(edda)]^-$. C_3 faces which are favorable for hydrogen bonding are indicated with arrows. (Modified from ref. 114.)

(iv) Kinetic detection of precursor ion-pair formation

Despite the difficulties involved in understanding the mechanisms of stereoselectivity in ion-pairing, the extensive data available allow valuable comparisons to be drawn with analogous electron transfer processes. One of the earliest reports [116,117] of electron transfer stereoselectivity provides an important contribution to the understanding of the role of the ion-pair. Stereoselectivity in the oxidation of the molybdenum(V) dimer,

$[\mathrm{Mo_2^VO_4}(R,S\text{-pdta})]^{2-}$, by the μ-superoxo complex, $[\Delta\Delta(\mathrm{en})_2\mathrm{Co}\text{-}(\mu\mathrm{NH_2,O_2^-})\mathrm{Co(en)_2}]^{4+}$

$$[\mathrm{Mo_2^VO_4}(R,S\text{-pdta})]^{2-} + 2[\Delta\Delta\text{-}(\mathrm{en})_2\mathrm{Co}(\mu\mathrm{NH_2,O_2{}^-})\mathrm{Co(en)_2}]^{4+} \rightarrow 2[\Delta\Delta\text{-}(\mathrm{en})_2\mathrm{Co}(\mu\mathrm{NH_2,O_2{}^{2-}})\mathrm{Co(en)_2}]^{3+} + 2\mathrm{Mo^{VI}(pdta)} \quad (23)$$

detected by monitoring optical activity in an excess of the racemic reductant, is small and is sensitive to ionic strength (Table 18). Limiting kinetic behavior in the reaction is consistent with the detection of a precursor complex and allows the determination of both the complexation constant and the electron transfer rate. The decrease in K_{ip} and increase in k_{et} with increasing ionic strength reflect a change in stereoselectivity from the *R* to the *S* isomer and it is concluded that the two steps have opposite selectivities, and that while $K_{ip}(\Delta\Delta\text{-}R)/K_{ip}(\Delta\Delta\text{-}S) > 1.09$, $k_{et}(\Delta\Delta\text{-}S) > k_{et}(\Delta\Delta\text{-}R)$. By way of explanation, it is proposed that the μ-superoxo O–O axis approaches perpendicular to the Mo–Mo axis in the electron transfer precursor with a preference for the *R*-pdta isomer but that the outer-sphere rearrangement required to attain the transition state for electron transfer is greater for this diastereomer than for the *S*-pdta diastereomer with the result that the intrinsic electron transfer rates show the opposite order.

There is an alternative explanation, that the kinetically detected ion pair is in fact, a 'dead-end' complex and that the electron transfer process requires a completely different geometry. In fact, the difference between the two explanations is largely semantic.

(v) The effects of added ions

The study of the effect of added ions on the stereoselectivity of a reaction has potential for providing details on the mediating role of these ions in the overall electron transfer reaction. Early outer-sphere electron transfer reac-

TABLE 18

Ionic strength dependence for the oxidation of $[\mathrm{Mo_2^VO_4}(R,S\text{-pdta})]^{2-}$ by $[\Delta\Delta\text{-}(\mathrm{en})_2\mathrm{Co}(\mu\mathrm{NH_2,O_2^-})\mathrm{Co(en)_2}]^{4+}$ at pH 4.6 and 25°C

μ (M)	k_{et} ($\mathrm{s^{-1}}$)	K_{IP} ($\mathrm{M^{-1}}$)	e.e. (%)
0.2	7.6×10^{-3}	51	0.15 (*R*)
0.35			0.036 (*R*)
0.50	9.9×10^{-3}	27	0
1.00	1.20×10^{-2}	18	0.13 (*S*)
1.50			0.20 (*S*)
2.00	1.7×10^{-2}	11	0.25 (*S*)

tions showed evidence for specific and general cation effects. This suggested that effects on reaction rates may be due either to incorporation of the ion into the activated complex, or that it simply has a general influence on the activity coefficients of the separated reactants as well as when in the activated complex [1]. Although initial reports indicated [57,58] a strong effect of PO_4^{3-} on chiral induction in the oxidation of $[Co(en)_3]^{2+}$ by $[Co(edta)]^-$, these are incorrect and the effects on this reaction of all ions so far investigated are minor [60]. In general, they have little effect beyond changing the distribution of conformational isomers [104].

One important series of reactions has been carried out by Saito and coworkers [118]. Chiral induction is detected in the oxidation of the molybdenum(V) dimer $[Mo_2O_4(R,S\text{-pdta})]^{2-}$ by $[IrCl_6]^{2-}$ when carried out in the presence of optically active metal ion complexes (Table 19). The absolute configuration of the added complex appears to direct the selectivity, and a mechanism involving reactive ion multiplets is proposed. This is a fairly general phenomenon. In the $[IrCl_6]^{2-}$ oxidation of $[Co(edta)]^{2-}$, a 2% excess of $[\Delta\text{-}Co(edta)]^-$ is induced in the presence of $[\Lambda\text{-}Co(en)_3]^{3+}$, the result of preferential ion pairing. Selectivity is enhanced to 7% with $[Co(sep)]^{3+}$, and is retained when $[Co(pdta)]^{2-}$ is oxidized, indicating that a Pfeiffer effect is not the operating mechanism [119].

Early work of Dwyer and coworkers [120] indicated the thermodynamic consequences of chiral electrolytes on the reduction potential of Δ-and Λ-$[Os(bpy)_3]^{3+}$. Effects on the order of 30 mV are observed in the presence of ammonium (+)-camphorsulphonate, and the chiral cation $[\Lambda\text{-}Co(en)_3]^{3+}$ also discriminates between the enantiomers. Kinetic stereoselectivity in electrode reactions has also been examined successfully. In the presence of chiral amine salts such as (−)-*N*,*N*′-tetramethylene-bis(dimethylmenthylammonium)diperchlorate, the rate of reduction of $[\Delta\text{-}Co(acac)_3]$ at a mercury electrode in acetonitrile solution is 1.10 times the rate of reduction of $[\Lambda\text{-}Co(acac)_3]$ [121,122]. More recently, liquid crystals have been used as a chiral medium in an examination of the $[Ru(bpy)_3]^{3+/2+}$ couple in acetonitrile [123].

TABLE 19

Effect of chiral complexes on the $[IrCl_6]^{2-}$ oxidation of $[Mo_2O_4(R,S\text{-pdta})]^{2-}$

Complex	e.e. (%)	Rate ratio (most reactive isomer)
$[\Lambda\text{-}Co(en)_3]^{3+}$	0.51	1.010 (*S*-pdta)
$[\Delta\text{-}Co(S\text{-}praH)(R\text{-}chxn)_2]^{3+}$	1.99	1.04 (*R*-pdta)
$[\Delta\text{-}Co(etaH)(R\text{-}chxn)_2]^{3+}$	0.15	1.003 (*R*-pdta)
$[\Delta\text{-}Co(gly)(en)_2]^{3+}$	0.07	1.001 (*R*-pdta)
$[\Lambda\text{-}Co(gly)(en)_2]^{3+}$	0.04	1.001 (*S*-pdta)

F. CHELATE RING CONFORMATION IN ELECTRON TRANSFER REACTIVITY

Chelate ring conformation has an important role in determining the stereochemical course of the reactions in the reactions involving strong hydrogen-bonding discussed in Sect. E. It can also have a profound effect on the reactivity of the metal ion complex. Recent work has focussed on both kinetic and thermodynamic aspects and it is of some interest to consider these features in relation to stereoselectivity.

The labile tris-bidentate chelate cobalt(II) reactants exist as equilibrium mixtures of the four conformational isomers, *lel*$_3$, *lel*$_2$*ob*, *lelob*$_2$, and *ob*$_3$ and there have been a number of experimental [124,125] and computational [126,127] determinations of the distribution of isomers. For $[Co(en)_3]^{2+}$, the dominant isomer is *lel*$_2$*ob* while for both $[Co(sen)]^{2+}$ and $[Co(sep)]^{2+}$, *lel*$_3$ forms are preferred [126]. Complexes with C-substituted ligands are conformationally restricted and for the inert cobalt(III) complexes the diastereomers are separable [58,128–130] (Table 20). Distributions of the diastereomers in the labile reduced cobalt(II) forms of the complexes are expected to differ from those of cobalt(III). The distribution of products in oxidations by $[Co(edta)]^-$, $[Co(ox)_3]^{3-}$, and $[Co(mal)_3]^{3-}$ will reflect the distribution of the reduced complex modified by differences in the electron transfer reactivity of the isomers (Table 21).

Bond et al. [131] have considered conformation effects on the reduction potentials in the $[Co((\pm)\text{-pn})_3]^{3+/2+}$ system and suggest that they cover a narrow range of 20 mV. Sargeson and coworkers [132] find that the self-exchange rate for the *lel*$_3$ isomer of $[Co\{(NH_3)_2,Me_3sar\}]^{5+/4+}$ is almost two orders of magnitude smaller than that for the *ob*$_3$ isomer (Table 22). The reduction potential of the *lel*$_3$ isomer is 300 mV higher than that for the *ob*$_3$ isomer. This is consistent with the pattern of reactivity observed. Ring conformation effects on reactivity have also been noted in reactions of macrocyclic complexes [133].

The rigidity of the cobalt(II) sepulchrates allows investigation [134–137] of structural features (Fig. 19) on self-exchange reactivity (Table 22). The

TABLE 20

Equilibrium distribution of isomers for $[Co((\pm)\text{-bn})_3]^{3+}$, $[Co((\pm)\text{-chxn})_3]^{3+}$, $[Co((\pm)\text{-pn})_3]^{3+}$ at 100°C

	$[Co((\pm)\text{-bn})_3]^{3+}$	$[Co((\pm)\text{-chxn})_3]^{3+}$	$[Co((\pm)\text{-pn})_3]^{3+}$
lel$_3$	46.1	46.7	35.0
lel$_2$*ob*	34.9	34.7	41.1
lelob$_2$	15.2	14.3	18.0
ob$_3$	3.9	3.3	4.0

TABLE 21

Isomer distribution in the oxidations of $[Co((\pm)\text{-bn})_3]^{2+}$ and $[Co((\pm)\text{-chxn})_3]^{2+}$ in aqueous media

	Product (%)				
	$[Co((\pm)\text{-bn})_3]^{3+}$		$[Co((\pm)\text{-chxn})_3]^{3+}$		
	$[Co(edta)]^-$	$[Co(ox)_3]^{3-}$	$[Co(edta)]^-$	$[Co(ox)_3]^{3-}$	$[Co(mal)_3]^{3}$
lel$_3$	32	38	37	36	33
lel$_2$*ob*	41	39	36	44	39
lelob$_2$	22	19	19	18	22
ob$_3$	6	4	8	2	6

TABLE 22

Reduction potentials and self-exchange rates for sepulchrate derivatives at 25.0°C and 0.20 M ionic strength

Complex	E^0 (V vs. N.H.E.)	k_{11} ($M^{-1}\,s^{-1}$)	ΔH^*	ΔS^*	Ref.
$[Co(sep)]^{3+/2+}$	−0.30	5.1	9.6	−23	134
$[Co(azamesar)]^{3+/2+}$	−0.36	2.9	7	−18	134
$[Co(azacapten)]^{3+/2+a}$	0.01	4500	7	−18	135
$[Co(amsartacn)]^{3+/2+}$	−0.08	0.086			136
$[Co(amsartacn)H]^{4+/3+}$	0.07	0.040			136
$[Co(sar)]^{3+/2+}$	−0.43	2.1			41
$[Co\{(NH_3)_2sar\}]^{3+/2+}$	−0.32	0.05			41
$[Co\{(NH_3)_2sar\}H_2]^{5+/4+}$	0.03	0.024			41
$[Co\{(NH_3)_2char\}\text{-}lel_3]^{3+/2+}$	−0.35	1.0			137
$[Co\{(NH_3)_2char\}H_2\text{-}lel_3]^{5+/4+}$	−0.01	0.038			137
fac-$[Co\{(NH_3)_2,Me_3sar\}\text{-}lel_3]^{5+/4+}$	0.015	0.031			132
mer-$[Co\{(NH_3)_2,Me_3sar\}\text{-}lel_3]^{5+/4+}$	0.015	0.033			132
fac-$[Co\{(NH_3)_2,Me_3sar\}\text{-}ob_3]^{5+/4+}$	−0.29	0.97			132
mer-$[Co\{(NH_3)_2,Me_3sar\}\text{-}ob_3]^{5+/4+}$	−0.32	1.00			132

[a] Low-spin cobalt(II).

effects of the C_3 cap and of bulky cyclohexane rings in the C_2 plane of the complexes is minor in comparison with the effects of charge and spin state. Stereoselectivity has also been detected [132,138] by rate comparisons for a number of reactions (Table 23). Ring conformation is more important than the facial or meridional placement of methyl groups which in turn is more important than the absolute configuration (Fig. 20). Nevertheless, it is interesting to note that *fac*/*fac* and *mer*/*mer* reactions show a preference for ΔΔ interactions while *fac*/*mer* reactions show a preference for ΔΛ. The stereoselec-

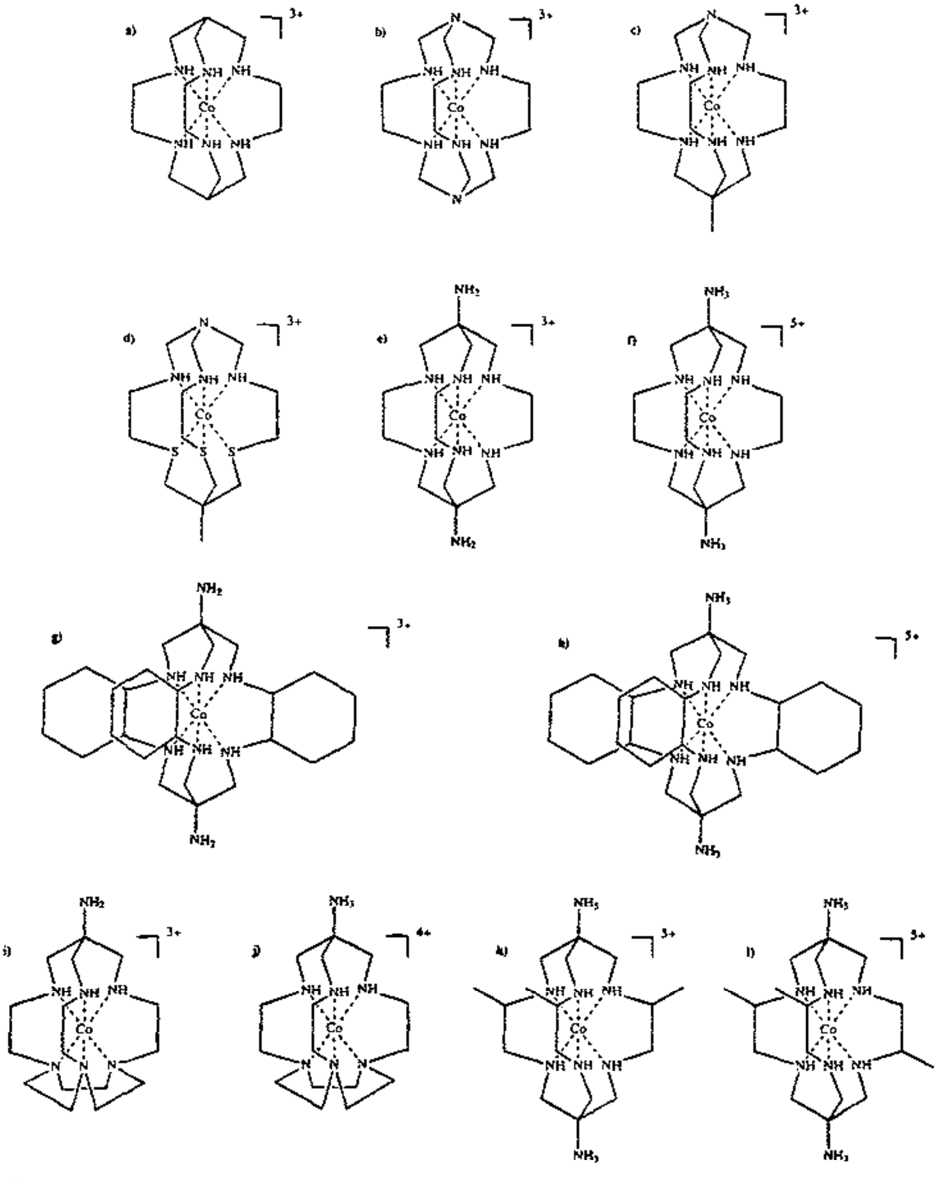

Fig. 19. Sepulchrate derivatives. (a) $[Co(sar)]^{3+}$; (b) $[Co(sep)]^{3+}$; (c) $[Co(azamesar)]^{3+}$; (d) $[Co(azacapten)]^{3+}$; (e) $[Co\{(NH_3)_2sar\}]^{3+}$; (f) $[Co\{(NH_3)_2sar\}H_2]^{5+}$; (g) $[Co\{(NH_3)_2char\}\text{-}\mathit{lel}_3]^{3+}$; (h) $[Co\{(NH_3)_2char\}H_2\text{-}\mathit{lel}_3]^{5+}$; (i) $[Co(amsartacn)]^{3+}$; (*j*) $[Co(amsartacn)H]^{4+}$; (k) *fac*-$[Co\{(NH_3)_2, Me_3sar\}\text{-}\mathit{lel}_3]^{5+}$; (l) *mer*-$[Co\{(NH_3)_2, Me_3sar\}\text{-}\mathit{lel}_3]^{5+}$.

tivities can be explained by steric effects from the methyl groups for interactions along the C_2 axis.

A corollary of the detection of stereoselectivity in these pseudo-self-exchange processes is the uncertainties introduced into self-exchange rates

TABLE 23

Rate and stereoselectivity data for reactions of sepulchrate derivatives at 25.0°C and 0.20 M ionic strenth [41, 132]

Reactants	k_{11} ($M^{-1}\,s^{-1}$)	$k_{\Delta\Lambda}/k_{\Delta\Delta}$
$[\Delta\text{-Co}\{(NH_3)_2\text{sar}\}]^{3+}$		
$[\Lambda\text{-Co(sep)}]^{2+}$	140	0.9
$[\Delta\text{-Co(sep)}]^{2+}$	156	
fac-$[\Delta\text{-Co}\{(NH_3)_2,\text{Me}_3\text{sar}\}\text{-}ob_3]^{4+}$		
mer-$[\Lambda\text{-Co}\{(NH_3)_2,\text{Me}_3\text{sar}\}\text{-}lel_3]^{5+}$	54	1.2
mer-$[\Delta\text{-Co}\{(NH_3)_2,\text{Me}_3\text{sar}\}\text{-}lel_3]^{5+}$	45	
fac-$[\Lambda\text{-Co}\{(NH_3)_2,\text{Me}_3\text{sar}\}\text{-}lel_3]^{5+}$	32	0.8
fac-$[\Delta\text{-Co}\{(NH_3)_2,\text{Me}_3\text{sar}\}\text{-}lel_3]^{5+}$	40	
mer-$[\Delta\text{-Co}\{(NH_3)_2,\text{Me}_3\text{sar}\}\text{-}ob_3]^{4+}$		
mer-$[\Lambda\text{-Co}\{(NH_3)_2,\text{Me}_3\text{sar}\}\text{-}lel_3]^{5+}$	14	0.8
mer-$[\Delta\text{-Co}\{(NH_3)_2,\text{Me}_3\text{sar}\}\text{-}lel_3]^{5+}$	17	
fac-$[\Lambda\text{-Co}\{(NH_3)_2,\text{Me}_3\text{sar}\}\text{-}lel_3]^{5+}$	13	1.3
fac-$[\Delta\text{-Co}\{(NH_3)_2,\text{Me}_3\text{sar}\}\text{-}lel_3]^{5+}$	10	

when measured by methods involving optical rotation. Examples are $[\text{Co(en)}_3]^{3+/2+}$, $[\text{Co(sep)}]^{3+/2+}$, and $[\text{Co(edta)}]^{-/2-}$. However, as with the $[\text{Co(phen)}_3]^{3+/2+}$ system [43] discussed in Sect. C (iii), provided the stereoselectivity is small, the errors are not serious.

G. REACTIONS OF METALLOPROTEINS

Reactions between metalloproteins are highly specific [139], the result of specific molecular interactions, and electron transfer reactions of metal-ion complexes with biological reagents are expected to show significant stereoselective behavior. Early work with intact organisms and protein extracts indicated that metal-ion complexes, particularly when used as the sole source of nitrogen, are metabolized stereoselectively [140–144]. Mechanistic studies with isolated proteins have also been carried out. Armstrong and Sykes [145] failed to detect differences in the rates of reduction of $[\Delta\text{-Co(en)}_3]^{3+}$ and *rac*-$[\text{Co(en)}_3]^{3+}$ by parsley ferredoxin. Cytochrome *c*(III), likewise, is reduced by $[\Delta\text{-Co(sep)}]^{2+}$ and $[\Lambda\text{-Co(sep)}]^{2+}$ at rates which are equal within experimental error [146].

The first reports of stereoselective electron transfer between metalloproteins involved differences in the rates of reduction of spinach plastocyanin by the chiral iron(II) reagents [Λ-Fe((*S*,*S*)-alamp)] and [Δ-Fe((*R*,*R*)-alamp)] (Fig. 21)

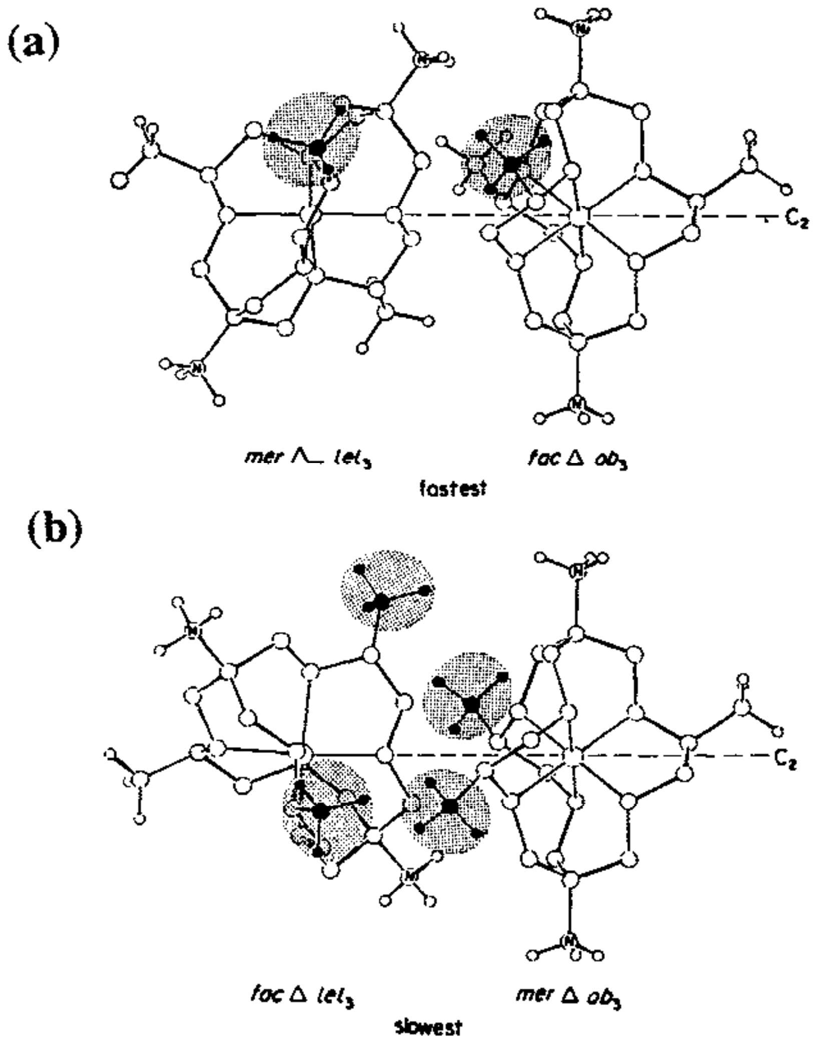

Fig. 20. Proposed orientations for ion association in electron transfer cross-reactions involving (a) *fac*-[Δ-Co{$(NH_3)_2$, Me_3sar}-*ob*$_3$]$^{4+}$ and *mer*-[Λ-Co{$(NH_3)_2$, Me_3sar}-*lel*$_3$]$^{5+}$, (b) *mer*-[Δ-Co{$(NH_3)_2$, Me_3sar}-*ob*$_3$]$^{4+}$ and *fac*-[Δ-Co{$(NH_3)_2$, Me_3sar}-*lel*$_3$]$^{5+}$. (Reproduced with permission from ref. 138 and based on data from ref. 132.)

[147]. Chiral induction is the result of differences in the activation entropies (Table 24). The reductants are labile and it is unclear whether the reactions are inner-sphere or outer-sphere. Spinach ferrodoxin is oxidized by the corresponding optically active cobalt(III) reagents in outer-sphere reactions which exhibit stereoselectivity [148]. In this case, strong temperature dependencies of the stereoselectivity give information on the relative importance of chiral recognition (identified with $\Delta\Delta H^{*}$) in the chiral induction.

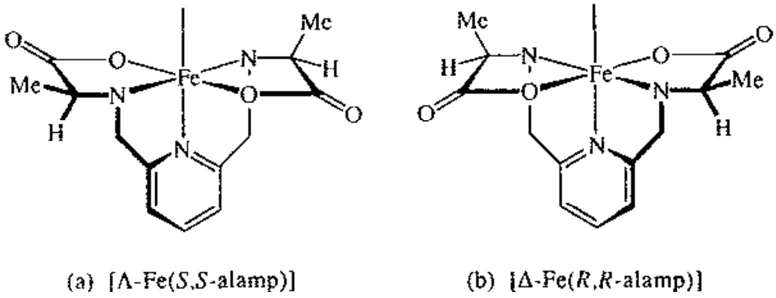
(a) [Λ-Fe(S,S-alamp)] (b) [Δ-Fe(R,R-alamp)]

Fig. 21. Structures of (a) [Λ-Fe(S,S-alamp)] and (b) [Δ-Fe(R,R-alamp)].

Chiral induction in the reduction of [Co(acac)$_3$] by horse cytochrome *c*(II) has been investigated [149]. Stereoselectivity in aqueous solution is small but is enhanced on addition of ethanol, the result of changes at the active site of the protein. Ionic strength and pH effects are interpreted in terms of participation of ion-pairing and hydrogen bonding in the reaction. The corresponding reaction with $[Co(ox)_3]^{3-}$ shows no dependence on pH [150]. At pH 7.0, partial reduction of *rac*-$[Co(ox)_3]^{3-}$ (in excess) by horse cytochrome *c*(II), results in an enantiomeric excess around 10% of the $[\Delta\text{-}Co(ox)_3]^{3-}$ isomer in solution. The $[\Lambda\text{-}Co(ox)_3]^{3-}$, therefore, reacts preferentially and the difference is large enough to allow kinetic detection [151]. Interpretation of the data is aided by the observation that chiral recognition between the oxidized protein and $[Co(ox)_3]^{3-}$ shows a similar preference for the Λ-isomer. Three binding sites for $[Co(ox)_3]^{3-}$ have been identified on the protein surface by NMR relaxation experiments with $[Cr(ox)_3]^{3-}$ as a paramagnetic probe [152], and from the absence of a phosphate dependence on the stereoselectivity, one of these is tentatively identified as the site of electron transfer (Fig. 22).

The stereospecific interaction of chiral metal phenanthroline complexes with DNA [153,154] has provided an interesting area for the study of stereoselective electron transfer. Electron transfer quenching of $[^*Ru(phen)_3]^{2+}$ by $[Co(bpy)_3]^{3+}$ is catalyzed by DNA, and the more tightly bound Δ isomer is quenched more rapidly [155,156]. A value for $k_\Delta/k_\Lambda \approx 1.75$ is obtained, larger than the stereoselectivity obtained in this reaction in the absence of DNA.

H. REACTIONS WITH NON-METALLIC SUBSTRATES

A number of workers have examined the effect of chiral transition metal ion complexes on the oxidation of optically active catecholates such as L-dopa. Early work by Shibata et al. [157,158] described stereoselectivity in

TABLE 24

Stereoselectivity in electron transfer reactions of metalloproteins, pH 7.0, $\mu = 0.1$ M

Reaction		k ($\mathrm{M^{-1}\,s^{-1}}$)	k_Δ/k_Λ	ΔH^* ($\mathrm{kcal\ mol^{-1}}$)	ΔS^* ($\mathrm{cal\ K^{-1}\,mol^{-1}}$)
Cytochrome *c*(III)	$[\Lambda\text{-Co(sep)}]^{2+}$	2.6×10^{-3}	1.08		
Cytochrome *c*(III)	$[\Delta\text{-Co(sep)}]^{2+}$	2.8×10^{-3}			
Plastocyanin(II)	$[\Lambda\text{-Fe}((S,S)\text{-alamp})]$	2.4×10^{4}	1.63	15.1	−109
Plastocyanin(II)	$[\Delta\text{-Fe}((R,R)\text{-alamp})]$	3.9×10^{4}		18.1	−94
Ferredoxin(III)(II)	$[\Delta\text{-Co}((R,R)\text{-alamp})\text{py}]$	6.1×10^{4}	1.27	19.8	−87
Ferredoxin(III)(II)	$[\Lambda\text{-Co}((S,S)\text{-alamp})\text{py}]$	4.8×10^{4}		31.6	−49
Ferredoxin(III)(II)	$[\Delta\text{-Co}((R,R)\text{-promp})\text{H}_2\text{O}]$	9.9×10^{4}	1.32	22.4	−73
Ferredoxin(III)(II)	$[\Lambda\text{-Co}((S,S)\text{-promp})\text{H}_2\text{O}]$	7.5×10^{4}		28.0	−56
Ferredoxin(III)(II)	$[\Delta\text{-Co}((R,R)\text{-promp})\text{py}]$	2.0×10^{5}	1.11	25.8	−56
Ferredoxin(III)(II)	$[\Lambda\text{-Co}((S,S)\text{-promp})\text{py}]$	1.8×10^{5}		25.8	−55
Cytochrome *c*(II)	$[\text{Co(acac)}_3]$		1.01		
Cytochrome *c*(II)	$[\Delta\text{-Co(ox)}_3]^{3-}$	4.28	0.89		
Cytochrome *c*(II)	$[\Lambda\text{-Co(ox)}_3]^{3-}$	4.81			

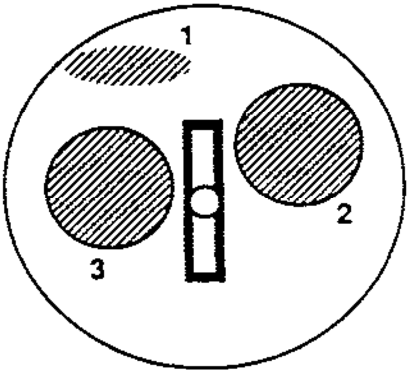

Fig. 22. Representation of cytochrome *c*, showing the heme edge and anion binding sites. Site 1 is on the top side of the protein, away from the heme edge; sites 2 and 3 are close to the heme edge. Site 3 is suggested to be the preferred site of binding and subsequent electron transfer for the $[Co(ox)_3]^{3-}$ oxidant. (Reproduced with permission from ref. 150.)

the autoxidation reaction catalyzed by Δ- and Λ-$[Co(en)_2(NH_3)Cl]^{2+}$, but their observations were subsequently shown to be subject to mis-interpretation [159]. However, stereoselectivity in the oxidation of $(+)_D$-catechin (3,3′,4′,5,7-flavapentol) was confirmed. A number of copper(II) complexes have also been employed as stereoselective catalysts in the oxidations of L-dopa and of sugars [160,161].

Pispisa and coworkers have carried out a series of detailed investigations of reactions catalyzed by $[trans\text{-}Fe(tetpy)(OH)_2]^+$ in poly(L-glutamate) or poly(D-glutamate) media. The metal complex is bound axially by the γ-carboxylate of two glutamate residues and this charge neutralization induces the formation of an α-helical structure [162]. The proportion of α-helix can thus be controlled by variation of the [complex]/[polymer] ratio or by variations in the pH. These assemblies catalyze the H_2O_2 oxidations of L-ascorbic acid [163–165], L-adrenaline [166–168], and L-dopa [167–169]

$$H_2O_2 + AH_2 \rightarrow A' + 2H_2O \tag{24}$$

where AH_2 is the reductant. At pH 7.0, the reaction kinetics are complex

$$\text{Rate} = k_{\text{uncat}}[H_2O_2][AH^-] + \frac{k_{\text{et}}K_o[\text{Fe(III)}][AH^-]}{(1 + K_o[AH^-])} \tag{25}$$

but are consistent with two pathways; an uncatalyzed pathway in which the rate-determining step is the reaction of H_2O_2 with the reductant, and a truly catalytic pathway in which the rate-limiting step involves direct interaction between the metal center and the reductant. The uncatalyzed pathway is accelerated by increasing α-helicity in the polypeptide, an effect of the polyelectrolyte, but the catalytic pathway is subject to retardation as a result of the steric factors introduced by the relatively compact α-helical arrangement. Interestingly, both pathways show stereoselectivity but it is much larger in the catalytic pathway and this latter pathway has attracted the most study. The stereoselectivity shows a linear dependence on the extent of α-helix formation and reaches an asymptotic value around four in all three reactions. All three reactions are considered to be outer-sphere in nature, but the reactions with L-adrenalin and L-dopa show kinetic evidence for a well-formed precursor complex [167,169] and this allows the separate determination of thermodynamic and kinetic components to the overall stereoselectivity (Table 25). The bulk of the stereoselectivity arises in the electron transfer step.

Detailed modelling studies [167,169,170] of the interactions between the α-helix bound iron(III) complex and the substrates have led to descriptions of the precursor complexes. These calculations are facilitated by the fact that many of the poorly defined quantities cancel on comparing the diastereomeric systems. The thermodynamic stereoselectivity results from the differences in electrostatic and non-bonding interactions in the diastereomeric pairs rather than a well-defined steric effect, and leads to good agreement with the experimental values. The differences in the electron transfer rate are explained by differences in the solvent polarization, although a contribution from electronic coupling cannot be excluded. Interestingly, the catalysis of the H_2O_2 oxidation of L-cysteine shows no chiral discrimination [171].

Other systems involving polypeptide bound metal ions have been shown to catalyze the autoxidation of L-dopa. When copper(II) is bound to poly(L-lysine) at pH 10.5, it shows stereoselectivity [172]. Although α-helical character is required for stereoselectivity, it is not a sufficient requirement and it is proposed that two different copper(II) centers are required for catalysis

TABLE 25

Limiting stereoselectivity in the oxidation of chiral catecholamines by polymer supported [*trans*-Fe(tetpy)]$^+$ at 25.9°C and pH 7.0

	k_{et} (s^{-1})	ΔH^*	ΔS^*	K_o (M^{-1})	ΔH°	ΔS°	$K_o k_{et}$
L-Dopa							
D	18.5×10^{-3}	17.4	−8	18.2×10^2	0.9	18	33.7
L	7.2×10^{-3}	17.5	−10	12.1×10^2	1.2	18	8.7
L-Adrenalin							
D	31.1×10^{-3}	16.6	−10	10.4×10^2	0.9	17	32.3
L	9.4×10^{-3}	16.6	−12	7.7×10^2	1.3	17	7.3
L-ascorbate							
D							414
L							106

[173,174]. The reaction is inner-sphere in nature and the stereoselectivity in this instance arises from discrimination in substrate binding with $K_L = 4.4 \times 10^3\ M^{-1}$, and $K_D = 6.5 \times 10^3\ M^{-1}$. The intrinsic rate of electron transfer within the precursor assembly shows no discrimination [172,175].

Reductive quenching of $[^*Ru(bpy)_3]^{2+}$ has also been featured in reactions with non-metallic substrates. Rau and Ratz [176,177] indicate that selectivity in the reaction with the chiral viologen, 1-methyl-1′-[(3*S*)-(−)-3-pinanylmethyl]-4,4′-bipyridinium dichloride (Fig. 23), $k_\Lambda/k_\Delta = 1.95$, is lost in the competing back electron transfer and ion-pair dissociation reactions. Similar observations in organic systems indicate selectivity in exiplex formation [178,179].

I. INNER-SPHERE STEREOSELECTIVITY

In principle, it might be expected that the greater definition and specificity of inner-sphere electron transfer reactions might favor highly stereoselective processes. However, there are considerable experimental difficulties associated with the study of stereoselectivity in inner-sphere reactions, not the least of which is the prospect of maintaining chirality in a substitution labile complex. There are other problems too, including increased complexity in the interpretation of data since the rate-determining step is not nearly so easy to define as it is in outer-sphere reactions.

That stereoselectivity in inner-sphere reactions can be large is implied by the claim [180] of a stereospecific inner-sphere reduction of $[Co(NH(py)_2)_2(N(py)_2)]^{2+}$ by $[Co(NH(py)_2)_2(DMF)_2]^{2+}$, where $NH(py)_2$ is 2,2′-bipyridylamine, which proceeds by an amide bridging ligand. However, the system has not been examined in any detail, and there are alternative explanations.

Bernauer et al. have designed [181,182] chiral electron transfer reagents with optimized specificity in inner-sphere interactions. The pentadentate ligand structure leaves one labile coordination site for the bridging process on a face in which chirality is maintained by high stereoselectivity in binding by the optically active ligand. The reduction of $[Co(bamap)(OH_2)]^+$ by the three iron(II) derivatives $[Fe(bamap)(OH_2)]$, $[Fe(alamp)(OH_2)]$, and $[Fe(valmp)(OH_2)]$ show second-order kinetic behavior and the pH dependence

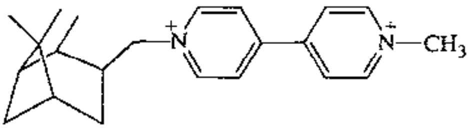

Fig. 23. Structure of 1-methyl-1′-[(3*S*)-(−)-3-pinanylmethyl]-4,4′-bipyridinium dichloride.

TABLE 26

Stereoselectivity in the reduction of $[Co(bamap)H_2O]^+$ by iron(II) complexes at 25.0°C

Reductant	$k_{\Delta\Lambda}/k_{\Lambda\Lambda}$	$\Delta\Delta G^*$ (kJ mol^{-1})
[Fe(bamap)]	1	0
[Fe(alamp)]	1.9	1.6
[Fe(valmp)]	1.2	0.45

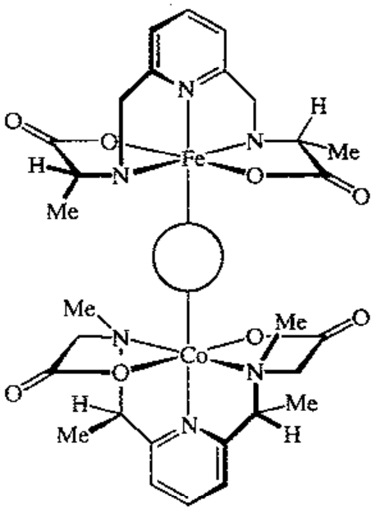

Fig. 24. Proposed transition state for the stereoselective inner-sphere electron transfer reaction involving [Λ-Co(*R*,*R*-bamap)$(OH_2)]^+$ and [Δ-Fe(*R*,*R*-alamp)(OH_2)]. (Modified from ref. 181.)

of the reaction gives evidence for an aquo-bridged intermediate. Stereoselectivities are monitored either by observing chiral induction in the unreacted excess oxidant, $[Co(bamap)(OH_2)]^+$, or by determining the individual rate constants for reactions of both enantiomers of the inert oxidant with the optically active reductant. Both methods give good agreement (Table 26). In all cases, the stereoselectivity is ΔΛ and molecular models, (Fig. 24) suggest that this is in keeping with the inner-sphere process, however definitive proof has not been obtained.

The discovery [105] of an inner-sphere pathway for the reduction of $[Co(ox)_3]^{3-}$ by $[Co(en)_2]^{2+}$ has prompted a study of the corresponding reactions of *N*-methyl substituted reductants [183]. Only one of the possible isomeric forms of $[Co(N,N\text{-}Me_2en)_2(ox)]^+$, with the substituted nitrogen atoms *trans* to each other, is obtained as a product and the chiral induction is 4.3% ΔΛ. Although three isomers of $[Co(N,N'\text{-}Me_2en)_2(ox)]^+$ are obtained, they are interconvertible in the basic conditions of the reaction and all show

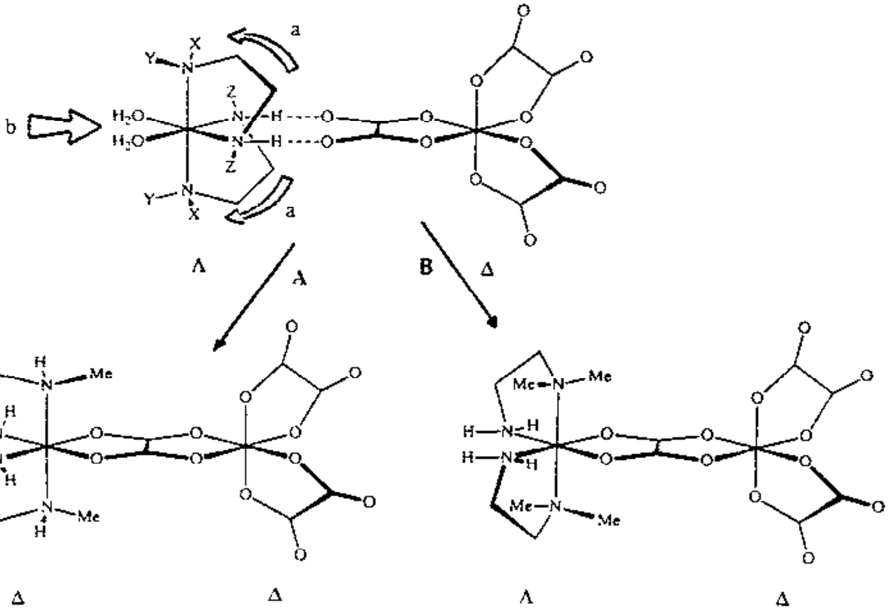

Fig. 25. Formation of the bridged binuclear intermediate from a hydrogen-bonded outer-sphere precursor in the reduction of $[Co(ox)_3]^{3-}$ by $[Co(en)_2]^{2+}$ and its derivatives. The outer-sphere precursor has a ΔΛ preference. When $X = H$; $Y,Z = H, CH_3$ inner-sphere association proceeds by solvent loss and inversion of configuration (arrows a) at the cobalt(II) center, pathway A, but this is prevented when $X,Y = CH_3$; $Z = H$, and reaction proceeds by attack on the reverse side of the reductant (arrow b) with retention, pathway B. (Reproduced with permission from *Inorganic Chemistry*.)

the same stereoselectivity, 7.9% ΔΔ, the same sense as that detected for the $[Co(en)_2(ox)]^+$ product. It is proposed that the sense is determined by the nature of a hydrogen-bonded outer-sphere precursor complex (Fig. 25). In the case of $[Co(N,N'\text{-}Me_2en)_2(ox)]^+$ and $[Co(en)_2(ox)]^+$, the product is obtained directly from this intermediate by inversion of the configuration at the labile cobalt(II) center whereas for $[Co(N,N\text{-}Me_2en)_2(ox)]^+$, the product is obtained by reaction on the opposite side of the reductant.

J. CONCLUSIONS

Over the past ten years, stereoselectivity in electron transfer reactions between metal-ion complexes has been established as a general phenomenon. It occurs even when electrostatic forces between the reactants are unfavorable. The stereoselectivities are not large, varying from vanishingly small to almost 80% enantiomeric excess, but are markedly dependent on the structures of the reactants, and provide a sensitive probe of mechanism. Interpretation of the data remains a difficulty. The role of precursor ion-pair structure, or chiral recognition, in determining chiral induction has been explored. It is important, especially where strong directional forces such as hydrogen bonds are involved, but it need be neither the exclusive nor the dominant source of the induction. Ion-pairs are dynamic, and a structure corresponding to favorable intermolecular interaction may not be favorable for electron transfer. Static structures such as those obtained from X-ray crystallography are interesting but may be misleading. Those obtained from model ion-pairing studies are thermodynamic averages of a dynamic system, and must be used with caution. Additional, electronic constraints for electron transfer which may be superimposed upon these dynamic structures are as yet unknown, but provide an important incentive for continuing efforts in this area. Recent work [184–186] on chiral discrimination in energy transfer between metal-ion complexes may provide additional information but appears to suffer from the same problems of interpretation as electron transfer studies.

Future work in this area will require careful examination of the energetics of the interactions involved in chiral induction. There are interesting developments in the interactions of metal-ion complexes with proteins and other biological materials, and in the dynamics of chiral processes at electrodes, and these provide new avenues for future research. Finally, the usefulness of spectroelectrochemical procedures in stereoselectivity studies has been noted [187,188] but has yet to be exploited.

K. LIST OF LIGAND ABBREVIATIONS

acacH	pentane-2,4-dione
β-alaH	β-alanine
($\pm$)-bn	*rac*-2,3-diaminobutane
bpy	2,2′-bipyridine
($\pm$)-chxn	*rac*-1,2-diaminocyclohexane
$R(+)$-cysu^{2-}	$R(+)$-cysteinsulfonate(2−)
cdta^{4-}	1,2-cyclohexanediamine-N,N,N',N'-tetraacetate(4−)
dmp	2,9-dimethylphenanthroline
edda^{2-}	ethylenediamine-N,N'-diacetate
edta^{4-}	ethylenediamine-N,N,N',N'-tetraacetate(4−)
en	1,2-diaminoethane
etaH	1-aminoethanol
glyH	glycine
ida^{3-}	iminodiacetate(3−)
mal^{2-}	malonate(2−)
[9]aneN_3	1,4,7-triazacyclononane
N,N-Me$_2$en	N,N-dimethyl-1,2-diaminoethane

N,*N'*-Me$_2$en	*N*,*N'*-dimethyl-1,2-diaminoethane
4,7-Me$_2$phen	4,7-dimethyl-1,10-phenanthroline
ox^{2-}	oxalate(2−)
pdta^{4-}	1,2-diaminopropane-*N*,*N*,*N'*,*N'*-tetraacetate(4−)
phen	1,10-phenanthroline
(±)-pn	*rac*-1,2-propanediamine
S-praH	(*S*)-2-aminopropanol
py	pyridine
sen	1,1,1-tris(((2-aminoethyl)amino)-methyl)ethane
sep	1,3,6,8,10,13,16,19-octaazabicyclo[6.6.6]eiosane
tetpy	2,2′:6′,2″:6″,2‴-tetrapyridine
tdta^{4-}	1,4-butanediaminetetraacetate(4−)
trdta^{4-}	trimethylenediaminetetraacetate(4−)

ACKNOWLEDGEMENT

The authors wish to acknowledge the support of the National Science Foundation (Grant No. 87–02012) in the preparation of this review.

REFERENCES

1 H. Taube, Electron Transfer Reactions of Complex Ions in Solutions, in E.M. Loebl (Ed.), Academic Press, New York, 1970.

2 A. Haim, Prog. Inorg. Chem., 4 (1983) 273.

3 E.S. Gould, Acc. Chem. Res., 18 (1985) 22.

4 R.A. Marcus, Annu. Rev. Phys. Chem., 15 (1964) 155.

5 N. Sutin, Acc. Chem. Res., 15 (1982) 275.

6 R.D. Cannon, Electron Transfer Reactions, Butterworths, London, 1980.

7 M.D. Newton and N. Sutin, Annu. Rev. Phys. Chem., 35 (1984) 437.

8 B.L. Tembe, H.L. Friedman and M.D. Newton, J. Chem. Phys., 76 (1982) 1490.

9 M.D. Newton, in The Challenge of *d* and *f* Electrons, D.R. Salahub and M.C. Zerner (Eds.), A.C.S. Symp. Ser. 394, A.C.S., Washington, DC, 1989, pp. 378–392.

10 G.M. Brown and N. Sutin, J. Am. Chem. Soc., 101 (1979) 883.

11 R.A. Marcus and N. Sutin, Biochim. Biophys. Acta, 811 (1985) 265.

12 J.K. Beattie, R.A. Binstead and M. Broccardo, Inorg. Chem., 17 (1978) 1822.

13 A.J. Miralles, R.E. Armstrong and A. Haim, J. Am. Chem. Soc., 99 (1977) 1416.

14 J. Phillips and A. Haim, Inorg. Chem., 19 (1980) 76.

15 A.J. Miralles, A.P. Szecsy and A. Haim, Inorg. Chem., 21 (1982) 697.

16 C.A. Koval, R.L.A. Pravata and C.M. Reidsema, Inorg. Chem., 23 (1984) 545.

17 P. Siders, R.J. Cave and R.A. Marcus, J. Chem. Phys., 81 (1984) 5613.

18 R.P. Domingue and M.D. Fayer, J. Phys. Chem., 90 (1986) 5141.

19 IUPAC Rule 7.8, Pure Appl. Chem., 28 (1971) 75.

20 The pairwise interactions are generally abbreviated by the dominant configuration. Thus, ΔΛΔ is abbreviated as Δ, and ΛΔΛ is abbreviated as Λ.

21 F.P. Dwyer and T.E. MacDermott, J. Am. Chem. Soc., 85 (1963) 2916.

22 Y. Saito, Top. Stereochem., 10 (1978) 95.
23 A. Adamson and S. Spees, Discuss. Faraday Soc., 29 (1960) 120.
24 B. Grossman and R.G. Wilkins, J. Am. Chem. Soc., 89 (1967) 4230.
25 A.M. Zwickel and H. Taube, Discuss. Faraday Soc., 29 (1960) 42.
26 W. Bruning and S.I. Weissman, J. Am. Chem. Soc., 88 (1966) 373.
27 R. Chang and S.I. Weissman, J. Am. Chem. Soc., 89 (1967) 5968.
28 J.H. Sutter and J.B. Hunt, J. Am. Chem. Soc., 91 (1969) 3107.
29 G.N. LaMar and G.R. Van Hecke, Inorg. Chem., 12 (1973) 1767.
30 N.A.P. Kane-Maguire, R.M. Tollison and D.E. Richardson, Inorg. Chem., 15 (1976) 499.
31 E.L. Blinn and R.G. Wilkins, Inorg. Chem., 15 (1976) 2952.
32 Z. Khurram, J.H. Espenson and A. Bakac, Inorg. Chem., 27 (1988) 3144.
33 K. Miyoshi, Y. Wada and H. Yoneda, Chem Lett., (1977) 319.
34 G.B. Porter and R.H. Sparks, J. Chem. Soc. Chem. Commun., (1979) 1094.
35 D.A. Geselowitz and H. Taube, J. Am. Chem. Soc., 102 (1980) 4525.
36 Y.A. Im and D.H. Busch, J. Am. Chem. Soc., 83 (1961) 3357.
37 H. Ogino and K. Ogino, Inorg. Chem., 22 (1983) 2208.
38 E. Blinn, C.F.V. Pearce and R.G. Wilkins, in M. Cais (Ed.), Progress in Coordination Chemistry, Elsevier, Amsterdam, 1968, pp. 135–137.
39 S. Harada, Y. Funaki and T. Yasunaga, J. Am. Chem. Soc., 102 (1980) 136.
40 F.P. Dwyer and A.M. Sargeson, J. Phys, Chem., 65 (1961) 1892.
41 I.I. Creaser, A.M. Sargeson and A.W. Zanella, Inorg. Chem., 22 (1983) 4022.
42 M. Micskei and I. Nagypál, J. Chem. Soc. Dalton Trans., (1990) 2581.
43 R.M.L. Warren, A.G. Lappin, B.D. Mehta and H.M. Neumann, Inorg. Chem., 29 (1990) 4185.
44 Y. Kaizu, T. Mori and H. Kobayashi, J. Phys. Chem., 89 (1985) 332.
45 L. Ørstrom and A.G. Lappin, unpublished results.
46 G.B. Porter and R.H. Sparks, J. Photochem., 13 (1980) 123.
47 E. Iwamoto, M. Yamamoto and Y. Yamamoto, Inorg. Nucl. Chem. Lett., 13 (1977) 399.
48 M. Yamamoto, E. Iwamoto, A. Kozasa, K. Takemoto, Y. Yamamoto and A. Tatehata, Inorg. Nucl. Chem. Lett., 16 (1980) 71.
49 E. Iwamoto, H. Saito and Y. Yamamoto, Polyhedron, 5 (1986) 815.
50 D.P. Craig and D.P. Mellor, Top. Curr. Chem., 63 (1976) 1.
51 R. Kuroda, S.F. Mason, C.D. Rodger and R.H. Seal, Chem. Phys. Lett., 57 (1978) 1.
52 R. Kuroda, S.F. Mason, C.D. Rodger and R.H. Seal, Mol. Phys., 42 (1981) 33.
53 K. Ohkubo, H. Ishida, T. Hamada and T. Inaoka, Chem. Lett., (1989) 1545.
54 K. Ohkubo, T. Hamada, T. Inaoka and H. Ishida, Inorg. Chem., 28 (1989) 2021, 3618.
55 K. Ohkubo and Y. Arikawa, J. Mol. Catal. 33 (1985) 65.
56 S. Sakaki, T. Satoh and K. Ohkubo, Nouv. J. Chim., 10 (1986) 145.
57 P. Osvath and A.G. Lappin, J. Chem. Soc. Chem. Commun., (1986) 1056.
58 P. Osvath and A.G. Lappin, Inorg. Chem., 26 (1987) 195.
59 D.A. Geselowitz, A. Hammershøi and H. Taube, Inorg. Chem., 26 (1987) 1842.
60 A. Tatehata and T. Mitani, Chem. Lett., (1989) 1167.
61 A.G. Lappin, M.C.M. Laranjeira and R.D. Peacock, Inorg. Chem., 22 (1983) 786.
62 D.P. Martone, P. Osvath, C. Eigenbrot, M.C.M. Laranjeira, R.D. Peacock and A.G. Lappin, Inorg. Chem., 24 (1985) 4693.
63 D.P. Martone, P. Osvath and A.G. Lappin, Inorg. Chem., 26 (1987) 3094.
64 M. Ishikawa, K. Okamoto, J. Hidaka and H. Einaga, Helv. Chim. Acta, 68 (1985) 2015.
65 Y. Masuda and H. Yamatera, Bull. Chem. Soc. Jpn., 57 (1984) 58.
66 Y. Masuda and H. Yamatera, J. Phys. Chem., 88 (1984) 3425.
67 D. Boys, C. Escobar and O. Wittke, Acta Crystallogr. Sect. C, 40 (1984) 1359.

68 R.D. Gillard, S.H. Mitchell and W.T. Robinson, Polyhedron, 22 (1989) 2649.
69 A. Yamagishi and M. Soma, J. Am. Chem. Soc., 103 (1981) 4640.
70 A. Yamagishi, Inorg. Chem., 25 (1986) 55.
71 A. Yamagishi, J. Coord. Chem., 16 (1987) 131.
72 A. Yamagishi and A. Aramata, J. Chem. Soc. Chem. Commun., (1984) 452.
73 A. Yamagishi, J. Coord Chem., 16 (1987) 131.
74 J.G. Mohanty, R. P. Singh and A. Chakravorty, Inorg. Chem., 14 (1975) 2178.
75 J.G. Mohanty and A. Chakravorty, Inorg Chem., 15 (1976) 2912.
76 J.G. Mohanty and A. Chakravorty, Inorg Chem., 16 (1977) 1561.
77 A.V. Ablov, N.I. Belichuk and V.N. Kaftanat, Russ. J. Inorg. Chem. (Engl. Transl.), 17 (1972) 392.
78 M. Mohapatra, V. Chakravorty and K.C. Dash, Polyhedron, 8 (1989) 1509.
79 J. Korvenranta, H. Saarinen and M. Näsäkkälä, Inorg. Chem., 21 (1982) 4296.
80 P.J. Heaney, A.G. Lappin, R.D. Peacock and B. Stewart, J. Chem. Soc. Chem. Commun., (1980) 769.
81 R.A. Marusak, C. Sharp and A.G. Lappin, Inorg. Chem., 29 (1990) 2298.
82 R.A. Marusak, C. Sharp and A.G. Lappin, Inorg. Chem., 29 (1990) 4453.
83 A.G. Lappin and M.C.M. Laranjeira, J. Chem. Soc. Dalton Trans., (1982) 1861.
84 A.G. Lappin and D.P. Martone, P. Osvath and R.A. Marusak, Inorg. Chem., 27 (1988) 1863.
85 F.P. Dwyer, E.C. Gyarfas and D.P. Mellor, J. Phys. Chem., 59 (1955) 296.
86 D.H. Busch, D.W. Cooke, K. Swaminathan and Y.A. Im, Adv. Chem. Coord. Compd., (1961) 139.
87 D.H. Busch, K. Swaminathan and D.W. Cooke, Inorg. Chem., 1 (1962) 260.
88 D.H. Busch and D.W. Cooke, J. Inorg. Nucl. Chem., 23 (1961) 145.
89 S. Kirschner, Y.-K. Wei and J.C. Bailar, J. Am. Chem. Soc., 79 (1957) 5877.
90 H. Irving and R.D. Gillard, J. Chem. Soc., (1961) 2249.
91 H. Irving and R.D. Gillard, J. Chem. Soc., (1960) 5266.
92 H. Ogino, M. Takahashi and N. Tanaka, Bull. Chem. Soc. Jpn., 43 (1970) 424.
93 F.P. Dwyer and F.L. Garvan, J. Am. Chem. Soc., 80 (1958) 4480.
94 M.K. Doh, H. Ogino, J. Fujita, K. Saito and N. Tanaka, Chem. Lett., (1974) 1233.
95 D.A. Geselowitz and H. Taube, Inorg. Chem., 20 (1981) 4036.
96 G.D. Armstrong, J.D. Sinclair-Day and A.G. Sykes, J. Phys. Chem., 90 (1986) 3805.
97 A.L. Poznjak, W.E. Stelmaschok, V.I. Pawlowski, E.B. Tschuklanowa, T.N. Polynowa and M.A. Porai-Koschitz, Z. Anorg. Allg. Chem., 499 (1983) 231.
98 U. Sakaguchi, I. Yamamoto, S. Izumoto and H. Yoneda, Bull Chem. Soc. Jpn., 56 (1983) 153.
99 U. Sakaguchi, I. Yamamoto, S. Izumoto and H. Yoneda, Bull Chem. Soc. Jpn., 56 (1983) 1407.
100 K. Miyoshi, Y. Sakamoto, A. Ohguni and H. Yoneda, Bull. Chem. Soc. Jpn., 58 (1985) 2239.
101 A. Tatehata, M. Fujita, K. Ando and Y. Asaba, J. Chem. Soc. Dalton Trans., (1987) 1977.
102 R.A. Marusak and A.G. Lappin, J. Phys. Chem., 93 (1989) 6856.
103 D.A. Young, T.B. Freedman, E.D. Lipp and L.A. Nafie, J. Am. Chem. Soc., 108 (1986) 7255.
104 A.G. Lappin, R.A. Marusak and P. Osvath, Inorg. Chem., 26 (1987) 4292.
105 R.A. Marusak, P. Osvath, M. Kemper and A.G. Lappin, Inorg. Chem., 28 (1989) 1542.
106 J.W. Vaughn, V.E. Magnuson and G.J. Seiler, Inorg. Chem., 8 (1969) 1201.
107 K.R. Butler and M.R. Snow, J. Chem. Soc. Dalton Trans., (1976) 251.
108 K. Miyoshi, Y. Sakamoto, Y. Toda and H. Yoneda, Bull. Chem. Soc. Jpn., 58 (1985) 1837.
109 K. Miyoshi, Y. Wada and H. Yoneda, Inorg. Chem., 17 (1978) 751.
110 K. Miyoshi, Y. Matsumoto and H. Yoneda, Inorg. Chem., 20 (1981) 1057.
111 H. Yamatera and M. Fujita, Bull. Chem. Soc. Jpn., 42 (1969) 3043.
112 H. Yokoyama, Bull. Chem. Soc. Jpn., 57 (1984) 1304.
113 A. Tatehata, M. Iiyoshi and K. Kotsuji, J. Am. Chem. Soc., 103 (1981) 7391.
114 A. Tatehata and Y. Asaba, Bull. Chem. Soc. Jpn., 61 (1988) 3145.
115 M. Kemper and A.G. Lappin, unpublished results.

116 K. Saito, in D. Banerjea (Ed.), Coordination Chemistry-20 (IUPAC), Pergamon Press, Oxford, 1980, pp. 173–181.

117 S. Kondo, Y. Sasaki and K. Saito, Inorg. Chem., 20 (1981) 429.

118 Y. Sasaki, K. Meguro and K. Saito, Inorg. Chem., 25 (1986) 2277.

119 P. Osvath and A.G. Lappin, unpublished observations.

120 G.T. Barnes, J.R. Backhouse, F.P. Dwyer and E.C. Gyarfas, J. Proc. R. Soc. N.S.W., 89 (1955) 151.

121 S. Mazur and K. Ohkubo, J. Am. Chem. Soc., 97 (1975) 2911.

122 K. Yoshinaga, T. Kito and K. Ohkubo, J. Chem. Soc. Jpn., (1986) 165.

123 R.D. Mariani and H.D. Abruna, J. Electrochem. Soc., 136 (1989) 113.

124 J.K. Beattie, Acc. Chem. Res., 4 (1971) 253.

125 C.J. Hawkins and J.A. Palmer, Coord. Chem. Rev., 44 (1982) 1.

126 A. M. Bond, T.W. Hambley and M.R. Snow, Inorg. Chem., 24 (1985) 1920.

127 K. Rasmussen, Potential Energy Functions in Conformational Analysis, Springer-Verlag, Berlin, 1985.

128 S.E. Harnung, B.S. Sørensen, I. Creaser, H. Maegaard, U. Pfenninger and R.C. Schäffer, Inorg. Chem., 15 (1976) 2123.

129 S.E. Harnung, S. Kallensøe, A.M. Sargeson, C.R. Schäffer, Acta Chem. Scand. Ser. A, 28 (1974) 385.

130 P.M. Hendry and A. Ludi, Adv. Inorg. Chem., 35 (1990) 117.

131 A.M. Bond, T.W. Hambley, D.R. Mann and M.R. Snow, Inorg. Chem., 26 (1987) 2257.

132 R.J. Geue, A.J. Hendry and A.M. Sargeson, J. Chem. Soc. Chem. Commun., (1989) 1646.

133 M.G. Fairbank, P.R. Norman and A. McAuley, Inorg. Chem., 24 (1985) 2639.

134 I.I. Creaser, R.J. Geue, J.M. Harrowfield, A.J. Herlt, A.M. Sargeson, M.R. Snow and J. Springborg, J. Am. Chem. Soc., 104 (1982) 6016.

135 R.V. Dubs, L.R. Gahan and A.M. Sargeson, Inorg. Chem., 22 (1983) 2523.

136 A. Hammershøi and A.M. Sargeson, Inorg. Chem., 22 (1983) 3554.

137 R.J. Geue, M.G. McCarthy and A.M. Sargeson, J. Am. Chem. Soc., 106 (1984) 8282.

138 A.M. Sargeson, Pure Appl. Chem., 58 (1986) 1511.

139 E. Cheung, K. Taylor, J.A. Kornblatt, A.M. English, G. McLendon and J.R. Miller, Proc. Natl. Acad. Sci. U.S.A., 83 (1986) 1330.

140 J. C. Bailar, H. Itatani, M.J.S. Crespi and J.F. Geldard, Adv. Chem., 62 (1967) 103.

141 R.D. Gillard and C. Thorpe, J. Chem. Soc. Chem. Commun., (1970) 997.

142 R.D. Gillard, J.R. Lyons and C. Thorpe, J. Chem. Soc. Dalton Trans., (1972) 1584.

143 C. Thorpe and R.D. Gillard, Biochim. Biophys. Acta, 392 (1975) 175.

144 L.S. Dollimore, R.D. Gillard and I.H. Mather, J. Chem. Soc. Dalton Trans., (1974) 518.

145 F.A. Armstrong and A.G. Sykes, J. Am. Chem. Soc., 100 (1978) 7710.

146 H.E. Toma and R.A. Murakami, Inorg. Chim. Acta, 93 (1984) L33.

147 K. Bernauer and J.-J. Sauvain, J. Chem. Soc. Chem. Commun., (1988) 353.

148 K. Bernauer, M. Monzione, P. Schürmann and V. Viette, Helv. Chim. Acta, 73 (1990) 346.

149 S. Sakaki, Y. Nishijima, H. Koga and K. Ohkubo, Inorg. Chem., 28 (1989) 4061.

150 R.A. Marusak, T.P. Shields and A.G. Lappin, in M.K. Johnson, R.B. King, D.M. Kurtz, C. Kutal, M.L. Norton and R.A. Scott (Eds.), Electron Transfer in Biology and the Solid State, American Chemical Society, Washington, DC, 1990 pp. 226, 237–252.

151 J. Ficke, J.R. Pladziewicz, E. Sheu and A.G. Lappin, to be published.

152 C.G.S. Eley, G.R. Moore, G. Williams and R.J.P. Williams, Eur. J. Biochem., 124 (1982) 295.

153 J. K. Barton and A.L. Raphael, Proc. Natl. Acad. Sci. U.S.A., 82 (1985) 6460.

154 J. K. Barton, Comments Inorg. Chem., 3 (1985) 321.

155 J. K. Barton, C.V. Kumar and N.J. Turro, J. Am. Chem. Soc., 108 (1986) 6391.

156 M.D. Purugganan, C.V. Kumar, N.J. Turro and J.K. Barton, Science, 241 (1988) 1645.

157 Y. Shibata and R. Tsuchida, Bull. Chem. Soc. Jpn., 4 (1929) 142.

158 Y. Shibata, Y. Tanaka and S. Goda, Bull Chem. Soc. Jpn., 6 (1931) 210.
159 Y. Yoshikawa and K. Yamasaki, J. Indian Chem. Soc., 54 (1982) 1250.
160 G. Losse, A. Barth and W. Langenbeck, Chem. Ber., 94 (1961) 2271.
161 N.K. Richtmyer and C.S. Hudson, J. Am. Chem. Soc., 58 (1936) 2540.
162 M. Branca and B. Pispisa, J. Chem. Soc. Faraday Trans. I, 73 (1977) 213.
163 M. Barteri, B. Pispisa and M.V. Primiceri, J. Inorg. Biochem., 12 (1980) 167.
164 M. Barteri and B. Pispisa, J. Chem. Soc. Faraday Trans. I, 78 (1982) 2073.
165 M. Barteri and B. Pispisa, J. Chem. Soc. Faraday Trans. I, 78 (1982) 2085.
166 B. Pispisa, M. Barteri and M. Farinella, Inorg. Chem., 22 (1983) 3166.
167 B. Pispisa, A. Palleschi, M. Barteri and S. Nardini, J. Phys. Chem., 89 (1985) 1767.
168 B. Pispisa, R. Rizzo, G. Paradossi and M. Marteri, J. Inorg. Biochem., 26 (1986) 281.
169 B. Pispisa and A. Palleschi, Macromolecules, 19 (1986) 904.
170 B. Pispisa, A. Palleschi and G. Paradossi, J. Phys. Chem., 91 (1987) 1546.
171 B. Pispisa, G. Paradossi, A. Palleschi and A. Desideri, J. Phys. Chem., 92 (1988) 3422.
172 T. Nozawa and M. Hatano, Makromol. Chem., 141 (1971) 21.
173 M. Hatano, T. Nozawa, S. Ikeda and T. Yamamoto, Makromol. Chem., 141 (1971) 1.
174 M. Hatano, T. Nozawa, S. Ikeda and T. Yamamoto, Makromol. Chem., 141 (1971) 11.
175 T. Nozawa and M. Hatano, Makromol. Chem., 141 (1971) 31.
176 H. Rau and R. Ratz, Angew. Chem. Int. Ed. (Engl.), 22 (1983) 550.
177 H. Rau, Chem. Rev., 83 (1983) 535.
178 M. Irie, T. Yorozu and K. Hayashi, J. Am. Chem. Soc., 100 (1978) 2236.
179 T. Yorozu, K. Hayashi and M. Irie, J. Am. Chem. Soc., 103 (1981) 5480.
180 Y.J. Wong, J.D. Petersen and J.F. Geldard, Inorg. Chem., 24 (1985) 3325.
181 K. Bernauer, P. Pousaz, J. Porret and A. Jeanguenat, Helv. Chim. Acta, 71 (1988) 1339.
182 K. Bernauer and P. Pousaz, Helv. Chim. Acta, 67 (1984) 796.
183 R.A. Marusak, M.A. Ivanca, K.J. Haller and A.G. Lappin, Inorg. Chem., 30 (1991).
184 D.H. Metcalf, S.W. Snyder, S. Wu, G.L. Hilmes, J.P. Riehl, J.N. Demas and F.S. Richardson, J. Am. Chem. Soc., 111 (1989) 3082.
185 D.H. Metcalf, S.W. Snyder, J.N. Demas and F.S. Richardson, J. Am. Chem. Soc., 112 (1990) 5681.
186 D.H. Metcalf, S.W. Snyder, J.N. Demas and F.S. Richardson, J. Phys. Chem., 94 (1990) 7143.
187 J. Daub, J. Salbeck and I. Aurbach, Angew. Chem. Int. Ed. Engl., 27 (1988) 291.
188 P.S. Braterman, B.C. Noble and R.D. Peacock, J. Phys. Chem., 90 (1986) 4913.